VRIJE UNIVERSITEIT AMSTERDAM
DELTARES

MASTER'S THESIS

Investigating the Implementation of Nature-Based Solutions in the Geul Catchment using Numerical Modelling

Author:
Huub Pieter KOPER

Supervisor:
Prof. Dr. Jeroen AERTS

Submitted to acquire the degree of
Master of Science in the field of
Hydrology

July 16, 2024

Abstract

Flash floods in rivers pose a significant threat to society and investigating measures to mitigate flood risk is therefore of vital importance. Nature-based solutions (NBS) are a novel approach to flood risk mitigation but research on the effects of NBS is still scarce. This research focuses on investigating the effects of different afforestation scenarios in the Geul catchment, a small cross-border catchment in the Netherlands, Belgium and Germany. The study uses the SFINCS hydrodynamic model to model the effects of the different afforestation scenarios on discharge and flood extent during the July 2021 extreme precipitation event, as well as several lighter (artificial) rainfall events (80% and 50% of the precipitation during the 2021 event). Results show that afforestation reduces the discharge largely proportional to the amount of forest cover added. However, results show only a limited effect on peak discharge for the more realistic afforestation scenarios (-0.7% to -2.6%). A delay in the peak discharge was also modelled; ranging from less than ten minutes for a lighter afforestation scenario to four and a half hours for a full afforestation scenario during the 2021 event. This could be useful for policymakers and/or flood preparedness in case of an event. A major flaw in the model arose when assessing the effect of afforestation on flood extent. In most scenarios, an increase of up to 8.8% was observed, where a decrease would be expected. This problem occurred because of the use of the curve number method for estimating runoff directly from precipitation. When using this method, water cannot infiltrate after the initial subtraction from the precipitation forcing, which results in an underestimation of the effectiveness of afforestation in the flood plain. Ultimately, SFINCS proved effective in modelling the flood extent of the July 2021 event at a low computation time, but using this model for investigating the implementation of nature-based solutions is not recommended.

Acknowledgements

I would like to thank prof. dr. Jeroen Aerts and dr. ir. Kymo Slager for their council during the writing of this thesis. Their thoughts and input were invaluable and really helped in the modelling and thesis writing process. I would also like to thank dr. Jens de Bruijn for his good suggestions in the modelling process and for his contributions to the scripts I have used. Special thanks in this goes out to Tarun Sadana for the use of his scripts and his great guidance in using SFINCS and Snakemake. Thank you for always being quick to answer and happy to help, without your help, this would have been a lot harder! I would also like to thank Romijn Servaas and Julius Overhoff, it was great being able to trade thoughts about our topics or results. Working on similar topics made the process of writing this thesis a lot more fun for me. Finally, I would like to thank the Institute for Environmental Studies and Deltares for allowing me to write my thesis on this interesting topic and as a part of the JCAR-ATRACE programme.

Contents

List of Figures

List of Tables

List of Abbreviations

AHN	**A**ctueel **H**oogtebestand **N**ederland
CN	**C**urve **N**umber
CSI	**C**ritical **S**ucces **I**ndex
ESA	**E**uropean **S**pace **A**gency
DEM	**D**igital **E**levation **M**odel
DWD	**D**eutscher **W**etter**d**ienst (German Weather Service)
ECMWF	**E**uropean **C**enter for **M**edium-**R**ange **W**eather **F**orecasts
ERA5	**E**CMWF **Rea**nalysis v**5**
FABDEM	**F**orest **A**nd **B**uildings removed Copernicus **DEM**
GCN250	**G**lobal Hydrologic **C**urve **N**umber **250**
GEV	**G**eneralized **E**xtreme **V**alue
GIS	**G**eographic **I**nformation **S**ystem
GloFAS	**Glo**bal **F**lood **A**wareness **S**ystem
GUI	**G**raphical **U**ser **I**nterface
HSG	**H**ydrologic **S**oil **G**roup
HydroMT	**Hydro** **M**odel **T**ools
HYSOGs250m	**Hy**drologic **So**il **G**roup**s250m**
KNMI	**R**oyal **N**etherlands **M**eteorological **I**nstitute
NAP	**N**ormaal **A**msterdams **P**eil (Dutch Ordnance Datum)
NBS	**N**ature-**b**ased **S**olutions
NetCDF	**Net**work **C**ommon **D**ata **F**orm
NRCS	**N**ational **R**esources **C**onservation **S**ervice
NSE	**N**ash-**S**utcliffe **e**fficiency
OET	**O**pen **E**arth **T**oolbox
RMSE	**R**oot **M**ean **S**quare **E**rror
SCS	**S**oil **C**onservation **S**ervice
SFINCS	**S**uper-**F**ast **IN**undation of **C**oast**S**
SSWE	**S**implified **S**hallow **W**ater **E**quations
QGIS	**Q**uantum **G**eographic **I**nformation **S**ystem
USDA	**U**nited **S**tates **D**epartment of **A**griculture

Chapter 1

Introduction

The Geul catchment is a small transboundary river catchment that covers parts of the border region of the Netherlands, Belgium, and Germany. The river has an average discharge of 4 m^3/s and acts as a tributary to the much larger Meuse river, which it enters in the town of Voulwames. In recent years, most notably in 2021, the Geul has been subjected to flash flooding (Slager et al., 2022; Van Heeringen et al., 2022). The 2021 flood event in particular has resulted in significant damages and a renewed interest in research on flood risk reduction measures to avoid situations like these in the future (Mohammed, 2022; Van Dijk, 2023; Middendorp, 2023; Idsinga, 2024), especially with respect to the expected increase in riverine flood risk due to climate change (Arnell and Gosling, 2016).

This chapter will discuss these flash floods, the event that occurred in July 2021, and how these floods are expected to increase in frequency and magnitude under climate change. Next, flood risk reduction methods, and in particular, nature-based solutions, will be discussed. This will then lead to the problem formulation and research question.

1.1 Flash floods in small rivers

Flash floods are a big concern in hydrology and hazard management because of the large number of people affected by them and the fact that they often result in fatalities (Marchi et al., 2010). These floods are caused by short, small-scale, but very intense rainfall events (Blöschl et al., 2015). The runoff response to these rainfall events is often less than six hours, and they mostly occur in small river catchments. The rapid response time makes these events particularly challenging from an early warning perspective, as the short lead time means that forecasting these events must strongly rely on meteorological forecasts (Brauer et al., 2011). Aside from the intensity of the rainfall, response dynamics are also influenced by various other factors, such as initial soil moisture conditions, topography and geology (Klein, 2022). An interplay of these factors resulted in floods in the various areas that were hit during the July 2021 event.

1.2 The July 2021 flood event

In the period from 12 to 15 July 2021, an extreme rainfall event took place in the border regions of Belgium, the Netherlands, Germany, and Luxembourg (Fig. 1.1). The intense rainfall led to floods in these regions, resulting in over 200 casualties and extensive infrastructural damage (Tradowsky et al., 2023). The rainfall itself was the result of a large low-pressure system over Central Europe that supplied warm and humid air masses to the region that was hit during this event. In the Geul catchment as a whole, this resulted in rainfall with a return period of roughly 500 years but in parts of the Ardennes, return periods exceeded 2500 years locally (Van Heeringen et al., 2022). In the Geul, the unprecedented amount of rainfall resulted in flash flooding conditions, and in the broader region there was severe flooding in North Rhine-Westphalia and Rhineland-Palatinate in Germany and along the river Meuse in Belgium and the Netherlands (Kreienkamp et al., 2021).

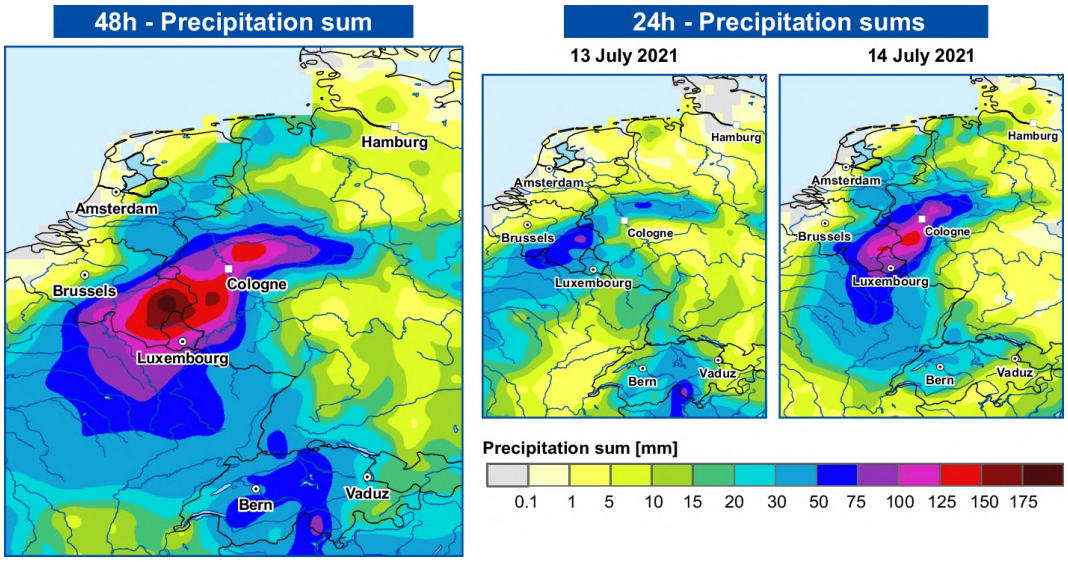

FIGURE 1.1: 48-hour (13 July 00:00 UTC - 15 July 00:00 UTC) and 24-hour precipitation sums over Central Europe for the extreme precipitation event. Taken from: Tradowsky et al. (2023).

1.3 Climate change

With a rise in global temperature, the hydrological cycle is expected to experience an intensification (Kundzewicz, 2008). This intensification is caused by the increase in evaporation of water under higher temperatures, which subsequently results in more rainfall too. This increase in rainfall is believed to result in more (extreme) floods as well (Milly et al., 2002). This is mostly true for rivers that are primarily fed by rainwater, as snowmelt-dominated catchments show a decrease in flood magnitude (Madsen et al., 2014). Because of climate change, events like the one in 2021 can occur more often; in 2050, these events can occur three times more often, and in 2085 up to six times more often (Asselman et al., 2022).

1.4 Flood risk reduction measures

This prospect has made research on measures to mitigate or reduce flood risk more relevant than ever. Traditionally, this field of study is focused on hard engineering or "grey" solutions. These measures include the construction of pipe networks, storage tanks, and flood walls/dikes (Kapetas & Fenner, 2020). However, the implementation of these measures is often costly and can lead to a technical lock-in.

A more novel approach to flood risk management is the implementation of so-called nature-based solutions (NBS). Nature-based solutions can be defined as “solutions that are inspired and supported by nature, which are cost-effective, and simultaneously provide environmental, social and economic benefits and help build resilience.” (European Commission, 2024). Within the fields of engineering and flood risk management, these types of solutions have garnered a lot of attention in recent years (Hartmann et al., 2019; Gottwald et al., 2021; Raška et al., 2022; Hugtenburg et al., 2023). A good example of this approach in the Netherlands is the Room for the River project. This project was initiated in 2007 and aims to reduce the flood risk in the large rivers of the Netherlands by literally giving the rivers more space by, for example, moving the dikes more inland (Rijke et al., 2012). By combining these measures with more traditional grey measures, the expected increase in flood risk due to climate change and population growth can be reduced more effectively.

1.5 Nature-based solutions

A variety of different nature-based solutions for flood risk mitigation exist, such as afforestation/reforestation to enhance evaporation and storage (Nadal-Romero et al., 2023), wetland restoration for more upstream storage (Gutman, 2019), and re-meandering to slow down discharge (Della Justina et al., 2019). Additionally, smaller-scale interventions have also been proposed as nature-based solutions, such as turning agricultural fields into natural grassland, creating infiltration strips, removing drainage pipes, and increasing the amount of green space in urban areas (Hugtenburg et al., 2023).

This research will focus on afforestation as a flood risk reduction measure. The increase in forest cover is thought to increase infiltration and evaporation, which reduces the amount of water that ends up in streams. Previous research has suggested that an increase in forest cover can reduce the flood risk (Bhattacharjee and Behera, 2018; Carrick et al., 2019; Buechel et al., 2022). Additionally, more forest cover can have a slowing effect on water, delaying the peak discharge but not always reducing the peak flow. It has also been suggested that the type of forest can have a major impact on its flood mitigation effectiveness. Tembata et al. (2020) suggest that deciduous and mixed forests have a flood mitigation effect, whereas forests with coniferous trees do not have a significant effect. Most research on the topic states that although afforestation can aid in reducing flood risk, it should be used in combination with traditional hard structural approaches (Calder & Aylward, 2006). This is especially true for more significant flood events as forest cover tends to have a limited effect on peak flows during extreme flood events (Bathurst et al., 2017; Xiao et al., 2022).

Aside from the reduction in flood risk, nature-based solutions like afforestation have a host of co-benefits. For example, converting agricultural land to forest can reduce soil erosion, nitrogen deposition, and pollution from pesticides, and it can also act as a carbon sink (Plantinga & Wu, 2003). It can also reduce the urban heat island effect when implemented in and around cities, while also improving water quality and increasing biodiversity. For humans, it can also create recreational areas and improve public health (Dittrich et al., 2019; Chakraborty et al., 2022). However, there are also potential trade-offs to implementing afforestation measures. One main downside is that it requires large amounts of land, which can come at the expense of, for example, agricultural land (Doelman et al., 2020). Additionally, other research has suggested that afforestation can also increase the vulnerability to droughts of downstream communities due to the heightened water consumption (Ward et al., 2020).

1.6 Problem statement and research objective

These challenges related to nature-based solutions, and afforestation in particular, highlight the importance of investigating where and to what extent afforestation can be implemented. However, research on the effectiveness of afforestation as a flood mitigation measure is still relatively scarce. Therefore, this research will focus on implementing different nature-based solutions in the form of afforestation scenarios into the hydrodynamic model SFINCS. Subsequently, the effectiveness of these measures will be assessed. This has not been done previously in this model, so part of the research will focus on how nature-based solutions can be implemented and whether it is viable for this type of model.

The main research question of this research is: **how can the 2D hydrodynamic model SFINCS be used to simulate the effects of implementing nature-based solutions in the Geul catchment to reduce flood risk?**
Additionally, several subquestions have been formulated to help answer this research question:

1. Is it possible to reproduce the flood situation in the Geul catchment during the July 2021 event with the SFINCS model?
2. How can the effects of nature-based solutions/afforestation be implemented into the SFINCS model?
3. What are the hydrological effects of implementing afforestation measures?
4. Is SFINCS a good model choice for this type of research?

Chapter 2 of this research will discuss the various aspects of the research area, after which the SFINCS model and the methodology will be discussed in Chapter 3. Subsequently, the results will be described in Chapter 4 and discussed in Chapter 5. Finally, the conclusions will be described in Chapter 6.

Chapter 2

Research area

The case study for this research focuses on the Geul catchment. The Geul is a transboundary river whose catchment area covers parts of the Netherlands, Belgium, and Germany (Fig. 2.1). The total catchment area is roughly 340 km^2, of which 52% is located in the Netherlands, 42% in Belgium, and 6% in Germany. The Geul is a tributary of the much larger Meuse river, which it joins north of the city of Maastricht in the Netherlands.

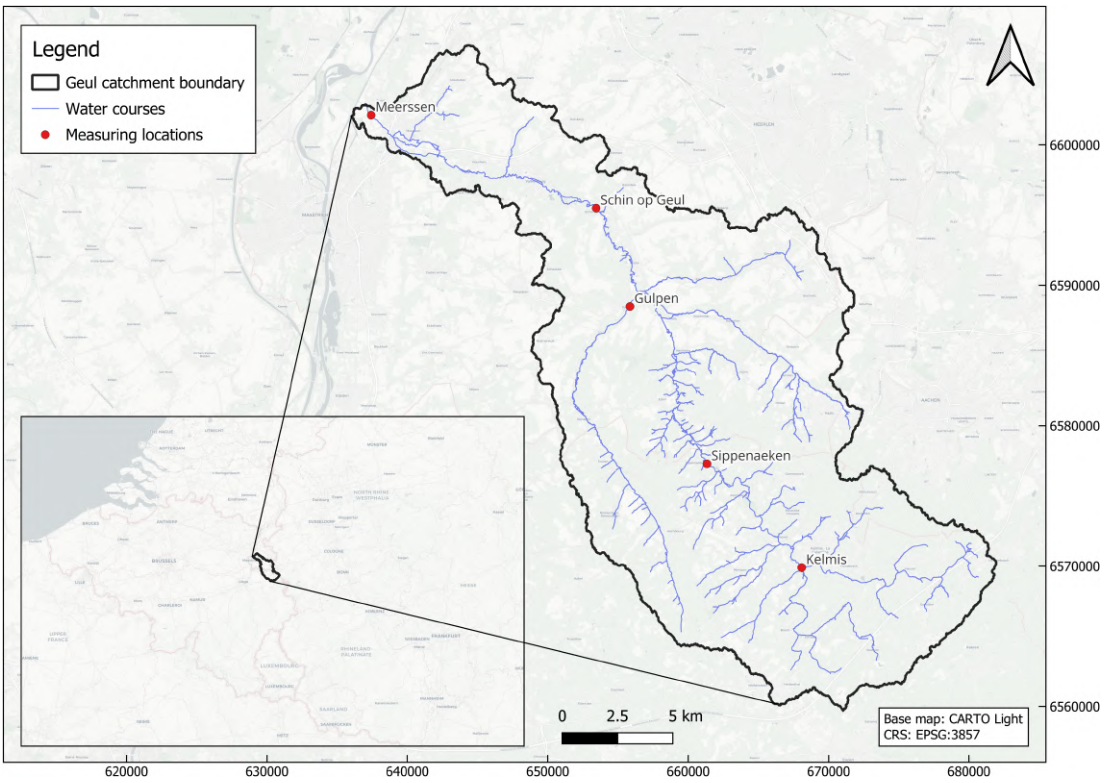

FIGURE 2.1: Location and catchment boundaries of the Geul catchment. The measuring locations are station locations of the water board, which are also used for validation in this research.

2.1 Topography

Figure 2.2 shows an elevation map of the Geul catchment. The elevation within the catchment varies between roughly 40 m and 370 m +NAP (Uhe et al., 2022). In the downstream part of the catchment, the river is deeply incised into the surrounding plateaus with steep slopes around the valley's edges. In the upstream part of the catchment, the river/tributaries are not as deeply incised into the plateaus, and the area is characterised by more gentle slopes. The stream gradient of the river itself is 4.3 m/km on average, but it should be noted that the stream gradient is significantly higher upstream of Gulpen when compared to downstream of Gulpen (Van Heeringen et al., 2022).

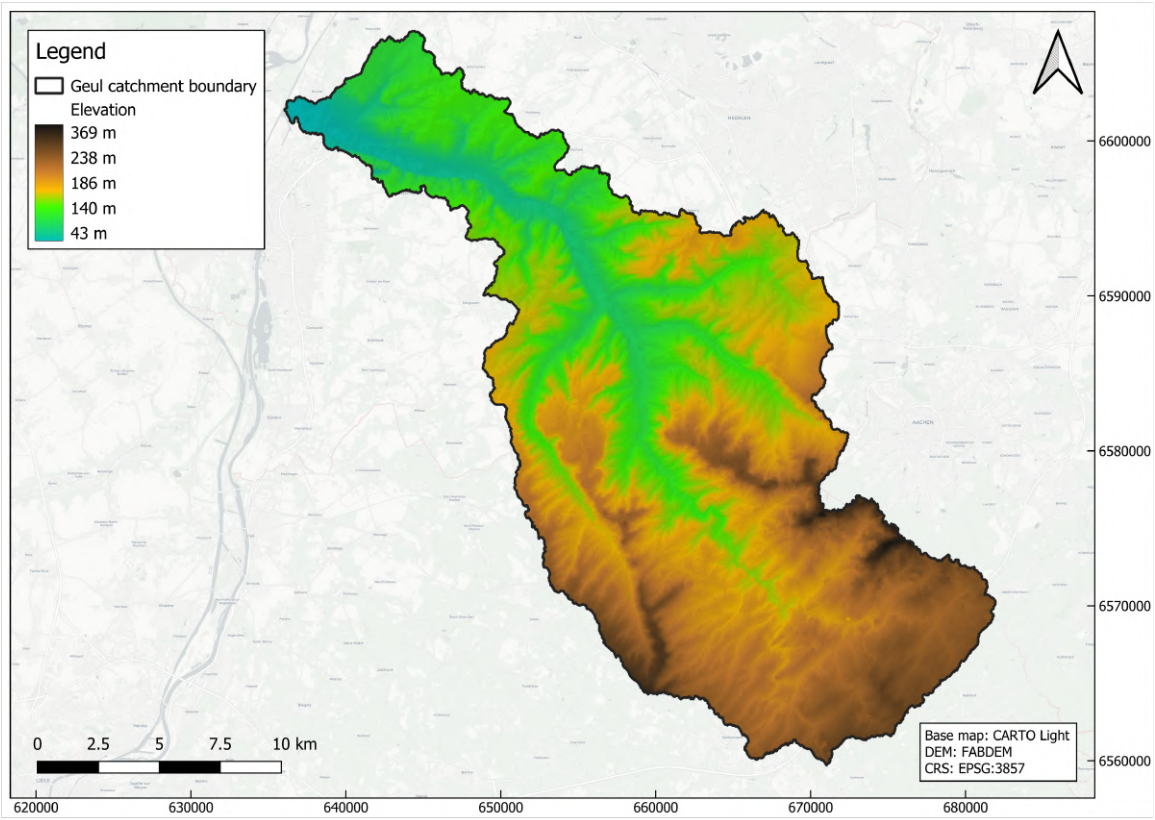

FIGURE 2.2: Elevation map of the Geul catchment.

2.2 Climate and hydrology

The Geul has an average discharge of approximately 4 m^3/s and it is a rainfed river. This means that the discharge can vary significantly depending on the rainfall conditions. In dry periods, the discharge can get lower than 1 m^3/s and in wet periods the discharge can reach up to dozens of m^3/s. The discharge is distributed throughout the year fairly evenly, which can be attributed to the release of water from the extensive chalk and limestone aquifers in the catchment area (Tu, 2006). The catchment is situated in a temperate oceanic climate (Cfb) according to the Köppen-Geiger climate classification (Kottek et al., 2006). This climate is characterised by a lack of significant differences in precipitation between seasons. However, the rainfall intensity is generally higher during the summer months. Average annual precipitation varies between 800 and 925 mm/year in the Dutch part of the catchment for the period 1991-2020, with the annual precipitation increasing towards the more elevated regions of the catchment (KNMI, 2024). The generally even distribution of precipitation and discharge throughout the year means that extreme discharges are generally caused by a combination of different factors. These factors include high precipitation, wet antecedent conditions, snow melt, and low evaporation/transpiration (Klein, 2022).

2.3 Geology

The geology in the south of Limburg is vastly different from the rest of the Netherlands. It is one of the few areas in the Netherlands where bedrock can be found this close to the surface, which greatly influences the hydrology in the area as well. Geologically, the

area belongs to the northern extensions of the Ardennes and the Eifel low mountain ranges (Hendrix & Meinardi, 2004). Within the catchment, significant variations in geology occur. In the most upstream (Belgian) part of the catchment, the oldest rock formations can be found at the surface, stemming from the Devonian and Carboniferous periods. These formations mostly consist of impermeable sandstones, slates, and hard limestones. Further downstream, younger rock formations from the Cretaceous period can be found. These include more permeable (clayey) sandstones and softer limestones. Younger deposits include sands and clays, of which the older Tertiary deposits can be compacted and impermeable. The youngest deposits in the area include loess deposits from the ice ages (mostly in the Dutch part of the catchment) and riverine deposits that were deposited by the Geul and its tributaries (Hugtenburg et al., 2023). Appendix B contains a map of the surface lithology in the region.

2.4 Land use

Table 2.1 shows the land cover distribution in the Geul catchment; a detailed land cover map can be found in Appendix B. Note that these land cover statistics were calculated using the ESA WorldCover 2021 v200 data set (Zanaga et al., 2022). Different land cover data sets will produce different results, as illustrated in Klein (2022). Throughout the history of the human settlement in the South of Limburg (roughly 7000 years), the landscape has changed drastically (De Moor et al., 2008). The most significant impact humans have had on the area is that of deforestation, often with the intent of creating arable land. Different deforestation phases were accompanied by an increase in soil erosion on the plateaus and slopes and more accumulation in the valleys. Over time, the landscape developed into a patchwork of woodland, pasture, and agricultural land, a so-called bocage landscape. In places where farmers left strips of woodland (at pasture edges for example), "graften" (escarpments) and "hollow roads" developed. The forest protected parts of the hills from erosion, creating lines along which the slope suddenly changes and, if roads went through these hedge-like woodlands, endeepened roads (Wallis de Vries, 2010).

TABLE 2.1: Land cover distribution in the Geul catchment. Data source: Zanaga et al. (2022)

Land Cover Class	**Percentage of Total Area**
Tree cover	30.3%
Grassland	43.8%
Cropland	18.5%
Built-up	7.2%
Permanent water bodies	0.1%

Chapter 3

Methodology

3.1 The SFINCS model

The SFINCS (Super-Fast INundation of CoastS) model is a two-dimensional hydrodynamic model developed by Deltares (Leijnse et al., 2021). The model solves the Simplified Shallow Water Equations (SSWE) with the aim of simulating compound flooding events. Compound flood events are, for example, events in coastal areas where the interaction of high sea levels, large river discharges, and local precipitation causes (extreme) flooding (Wahl et al., 2015). SFINCS was therefore initially developed with the aim of modelling coastal flood scenarios but it has since been applied to riverine flood scenarios as well. In fact, the model has been applied to various flooding scenarios since its initial development, such as urban flooding, riverine flooding, compound flooding, and tsunami modelling (Leijnse, 2024). One of the most useful features of the SFINCS model is the option to run the model in subgrid mode. In this mode, the flux calculations are carried out on a pre-defined, coarser, grid. The resulting water levels are then overlain on a finer resolution Digital Elevation Model (DEM) (Fig. 3.1). In doing so, computational times are decreased significantly while still using higher-resolution topographic data.

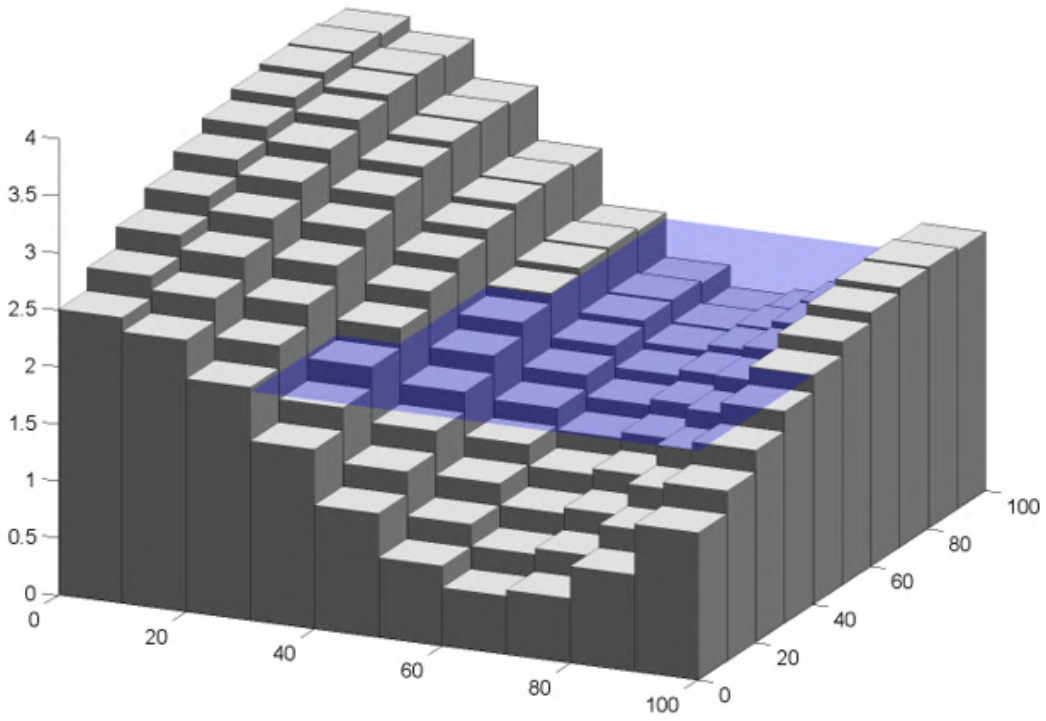

FIGURE 3.1: Representation of subgrid features. Flux computations are calculated on a coarser grid (blue) but water levels are updated on a finer resolution (grey). Source: Leijnse (2024)

Equations 3.1 and 3.2 show how the volumetric flow rate at the interface between adjacent cells is calculated in the x-direction and y-direction respectively. In these equations, $q^{t+\Delta t}$ is the volumetric flow rate at the next time step, q^t is the volumetric flow rate at the previous time step, g is the gravitational constant, h^t is the average water depth of the two adjacent cells, Δz is the water level difference between the cells, adv is the advective term, τ_w is the wind shear stress, ρ_w is the density of water, and n is Manning friction coefficient. Further information on how some of the terms in these equations are calculated can be found in Leijnse et al. (2021).

$$q_x^{t+\Delta t} = \frac{q_x^t - \left(g h_x^t \frac{\Delta z}{\Delta x} + adv_x - \frac{\tau_{w,x}}{\rho_w} \right) \Delta t}{1 + g \Delta t n^2 q_x^t / (h_x^t)^{7/3}} \tag{3.1}$$

$$q_y^{t+\Delta t} = \frac{q_y^t - \left(g h_y^t \frac{\Delta z}{\Delta y} + adv_y - \frac{\tau_{w,y}}{\rho_w} \right) \Delta t}{1 + g \Delta t n^2 q_y^t / (h_y^t)^{7/3}} \tag{3.2}$$

The SFINCS model can use various input files and settings and produce different outputs. In its most basic form, the model uses an input DEM and a type of forcing (water levels, discharge, or precipitation) to perform the flux calculations. The different input and output options will be discussed in more detail in the sections below. Additionally, the Python-based command-line way of using SFINCS (HydroMT-SFINCS) and Snakemake will be discussed, which were used to run the model for this research.

3.1.1 Model input

Figure 3.2 shows the various input files for the SFINCS model. The input can be divided into four categories: the files to set up the model domain, the model settings, the forcing files, and the structure files. For setting up a basic SFINCS model, few input files are required, but other input options exist for modelling more complex events. The choice of input files is dependent on the research at hand.

- **Model domain**: setting up the model domain is done using an input DEM and a file containing the outline of the research area. The DEM is then clipped to this outline. Other files are needed to specify the cell indexation (active, inactive, boundary, and outflow cells), this will be discussed in further detail in the section on HydroMT because this is done automatically in the setup used for this model. Further (optional) input files include land cover and curve number files to incorporate spatially varying roughness and infiltration, respectively. Finally, observation points and lines can be set up to record water depth and discharge respectively at specific points in the research area. Different resolutions are available for these input files, depending on the modeller's choice of data set but it should be noted that all of these data sets are resampled to the subgrid resolution. This means that a 30-meter DEM will be resampled to a 100-meter resolution to perform the flux calculations if this is the resolution that the subgrid is set to.
- **Model settings**: further model settings, like the time and output options, can be set separately. There are also several numerical parameters that can be adjusted to improve model stability, depending on the research at hand. All these settings can be changed in the overall input file (sfincs.inp).

- **Forcing**: forcing of the model is done using one of three types of forcing, or a combination of different forcing types. The main categories of forcing are water levels, discharges, and meteoric forcing. For this research, only gridded precipitation is used as forcing, but because SFINCS was originally developed as a (coastal) compound flooding simulator, additional forcing options exist for waves, air pressure, and wind.
- **Structures**: finally, options exist for incorporating several types of man-made structures into the model domain. These structures can be used to divert or block the flow of water, and can therefore be used to simulate flood hazard reduction methods (Leijnse, 2024). Three types of structures currently exist for use in the model: thin dams, weirs, and drainage pumps and culverts. These structures are snapped to the model grid and influence how the water flows. Thin dams and weirs can block water flow. Thin dams block all water flow ('unlimited height') whereas weirs block water flow up to a certain height. Pumps and culverts can divert water from one cell to the other. Pumps do so with a fixed discharge and culverts do so based on the water level gradient (but still with a maximum discharge). All of these structures represent traditional 'grey' infrastructure and therefore they will not be used in this model because the focus is on nature-based solutions.

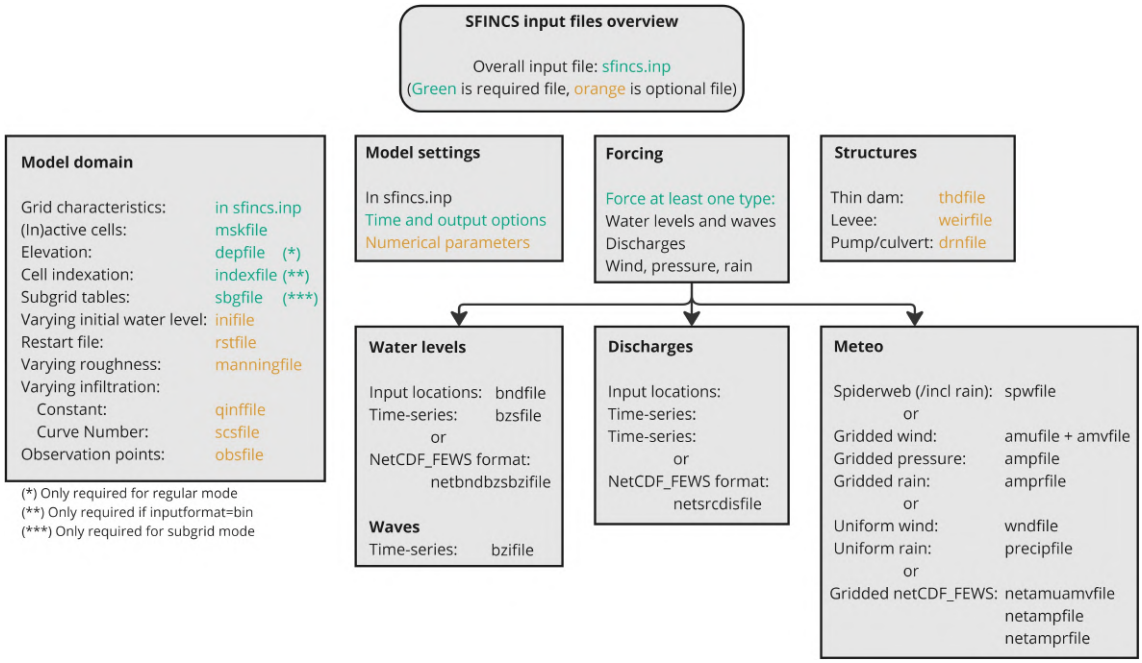

FIGURE 3.2: Overview of input files for SFINCS with an indication of whether they are required (green) or not (orange). Adapted from: Leijnse (2024)

3.1.2 Model output

The output of the SFINCS model consists of one or two NetCDF files that contain the model results: sfincs_map.nc and sfincs_his.nc. The SFINCS map file contains the global output of the model, including water depths and flow velocities at each time step, as well as maximum water levels for each previously defined time period. The (optional) sfincs_his file contains model results for specific locations. It contains similar outputs to the global output file, but now for the various point objects in the model domain, such as the discharge through pumps and culverts and the water levels and discharges at the defined observation points

and lines. Postprocessing of the output files and visualisation of the results can be done using a programming language such as Python and/or a geographic information system (GIS) of choice.

3.1.3 HydroMT and Snakemake

Several options exist for setting up a SFINCS model: the Delft Dashboard Graphical User Interface (GUI), the Matlab-based Open Earth Toolbox (OET), or the Python-based HydroMT-SFINCS. For this research, HydroMT (Hydro Model Tools) was used. HydroMT is a Python package that can be used to automate the building and analysis of geoscientific models (Eilander et al., 2023). The model-specific plugin HydroMT-SFINCS can be used to set up the SFINCS model by creating Python scripts that can automate many of the model preprocessing, model building, model running, and postprocessing steps. Using HydroMT-SFINCS, various model setup steps are completed for this research. For example, one of the main input files, the mask file (mskfile, Fig 3.2), is created by combining the catchment outline and river centerlines. This file specifies the model domain and outflow points of the catchment (for coastal models it has the additional function of setting water level boundary cells). Using the HydroMT-SFINCS package, scripts were created for building the model, implementing the forcing, running the model, postprocessing the results, and calculating model performance (Fig. 3.3).

To automate this workflow from pre-processing to calculating the model performance, Snakemake was used. Snakemake is a workflow management system that allows for a rule-based execution of the various scripts in a workflow (Mölder et al., 2021). By using this Snakemake setup, running the various scripts can be done in a more automated and reproducible way. It does so by having different 'rules' that break down the workflow into various smaller steps, which in this case correspond with the different scripts. When changes are made to a script or input file, the Snakemake workflow will detect these changes and run the workflow again starting from this point. This speeds up the workflow execution and reduces the risk of workflow errors.

3.2 Setting up the model for the 2021 event

Because this research concerns the headwater area of an inland river catchment, several components could be omitted from the model. Forcing consisted only of precipitation, as opposed to the multiple types of forcing in a compound flood event or an inland river catchment not located in the headwater area. Additionally, no structures such as dams and weirs were incorporated into the model because of the small scale of the catchment. Figure 3.3 shows the different scripts that were used in the Snakemake workflow, as well as the various input files that were used in the SFINCS model for this research.

3.2.1 Input data

The sections below will discuss the various data sets that were used to set up the model for the July 2021 event. Additionally, some of the data sets went through or were used for, pre-processing steps in Python or QGIS, these steps will also be discussed below.

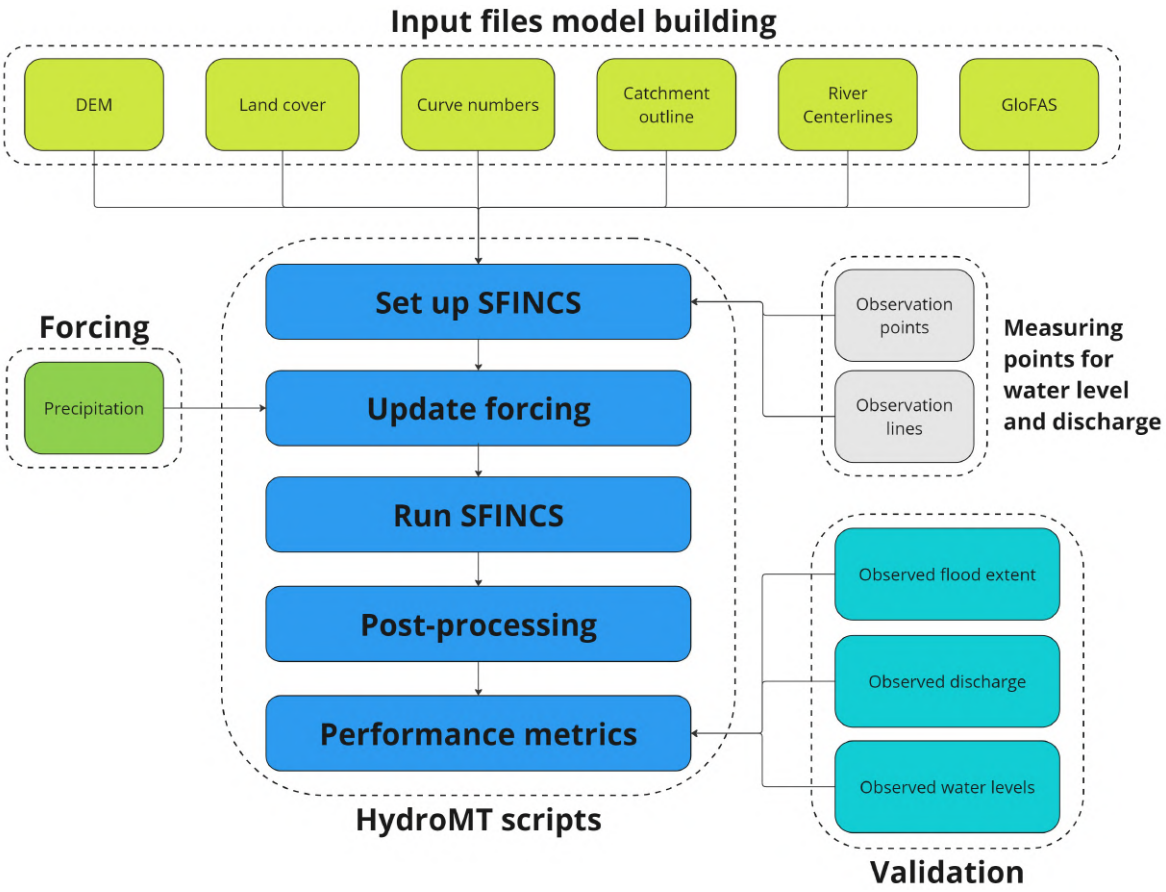

FIGURE 3.3: Overview of the different scripts and input files used to run the model for the Geul catchment.

3.2.1.1 Digital Elevation Model

For the topography of the catchment, the FABDEM data set was used. This is a global elevation data set derived from the Copernicus Digital Elevation Model where buildings and forests were removed using machine learning (Hawker et al., 2022). The data set has a 1 arc second resolution (~30 m at the equator) and the mean absolute vertical error is 1.12 m in built-up areas and 2.88 m in forests. Note that the model sub(grid) settings influence the final resolution in the model. For a 100 m grid resolution and 20 m subgrid resolution (used in this model), the DEM is resampled to these resolutions for the flux calculations and final water depth calculations respectively.

3.2.1.2 Land cover

For the land cover information of the catchment, the ESA WorldCover 10 m 2021 v200 data set was used. This data set provides a global land cover map for 2021 at a 10 m resolution based on Sentinel-1 and Sentinel-2 data (Zanaga et al., 2022). The data set is divided into 11 different land cover classes based on the Food and Agriculture Organization (FAO) of the United Nations' Land Cover Classification System (Di Gregorio, 2005). The land cover data set has been independently validated and was found to have a global overall accuracy of 76.7% (Tsendbazar et al., 2021), which should be considered when evaluating the model results. In the model itself, the 10 m resolution of the data set is resampled to a 20 m resolution in the subgrid mode.

This land cover data is used in the model to implement spatially varying surface roughness into the model. This is done by including a conversion table (Table 3.1) for converting the land cover classes to their corresponding Manning roughness coefficients, which represent surface roughness in s/m. These values are integrated into the momentum equations that SFINCS uses to calculate flow rates between grid cells (Equation 3.1 and 3.2). Note that Manning values for different land cover types vary throughout literature, so the choice of Manning values may influence the model results (Kalyanapu et al., 2009; Nyaupane et al., 2018).

TABLE 3.1: Land cover classes from the ESA WorldCover data set and corresponding Manning values used in SFINCS.

Land cover class	**Manning roughness (N)**
10 - Tree cover	0.120
20 - Shrubland	0.050
30 - Grassland	0.034
40 - Cropland	0.037
50 - Built-up	0.100
60 - Bare / sparse vegetation	0.023
70 - Snow and Ice	0.010
80 - Permanent water bodies	0.020
90 - Herbaceous wetland	0.035
95 - Mangroves	0.070
100 - Moss and lichen	0.025
0 - No data	-999

3.2.1.3 Curve numbers

Implementing infiltration into the model domain can be achieved in several ways. In more basic models, flat infiltration values or spatially varying infiltration values can be used. A slightly more involved method is the use of curve numbers (Cronshey, 1986). The Soil Conservation Service (SCS), now National Resources Conservation Service (NRCS), Curve Number (CN) method is an empirical method that describes the relationship between direct runoff volume and rainfall. The method was developed by the United States Department of Agriculture (USDA) (Singh and Mishra, 2003; Leijnse et al., 2021).

Curve numbers vary between different regions and are dependent on land cover, soil, treatment, and hydrologic conditions of the area. Look-up tables have been developed that give the curve numbers for various combinations of land cover and hydrologic soil group (HSG). These hydrologic soil groups were created for the curve number method and consist of soil classifications into four distinct groups: A, B, C, and D, which correspond to soils with low, moderately low, moderately high, and high runoff potential, respectively (Cronshey, 1986). Curve numbers vary between 30 (low runoff potential) and 100 (high runoff potential). Curve numbers are first converted to an S-value, which is the potential maximum soil moisture retention after runoff begins (Eq. 3.3). In this equation, CN is the curve number. The S-value is also used to determine the initial abstraction I_a, which are all water losses before runoff begins (Eq. 3.4). These include water retained in surface depressions, interception by vegetation, evaporation, and infiltration (Cronshey, 1986). These terms are then used to calculate the runoff (Eq. 3.5). The equation denotes that runoff is only generated when the initial abstraction value is exceeded. Note that all these equations use units of inches.

$$S = \frac{1000}{CN} - 10 \tag{3.3}$$

$$I_a = 0.2S \tag{3.4}$$

$$Q = \begin{cases} 0 & \text{for } P \leq I_a \\ \frac{(P-I_a)^2}{P-I_a+S} & \text{for } P > I_a \end{cases} \tag{3.5}$$

By default, SFINCS uses curve number maps from the GCN250 data set (Jaafar et al., 2019), which has a spatial resolution of 250 m and is based on gridded hydrologic soil groups at a 250 m resolution and land cover data at a 300 m resolution. For investigating the influence of afforestation on flood risk, a 300 m land cover map would not suffice. Therefore, a new curve number map was created for this research. The most detailed data set on hydrologic soil groups available for Europe is the HYSOGs250m data set, which was also used to create the GCN250 data set. For land cover, the ESA WorldCover data set was used but this leads to a problem because look-up tables for curve numbers only exist for the United States National Land Cover Database (NLCD). Therefore, the land cover classes from the ESA Worldcover data set were linked to corresponding land cover classes in the NLCD 2019 data set (Wickham et al., 2023) as shown in Table 3.2.

Because of the high spatial resolution of the ESA WorldCover data set, most "Built-up" areas in the catchment fall under the "Developed, High Intensity" classification of the NLCD 2019 data set (Wickham et al., 2023). Therefore, these curve numbers were taken for the built-up area part of the catchment. For forests, detailed land cover maps of the Netherlands show a mixed distribution of deciduous and coniferous forests in the area (Hazeu et al., 2023). Therefore, the values for "Mixed Forest" were taken for this land cover type. This assumption can influence the final results, and this should therefore be taken into account when evaluating the model results.

Finally, QGIS was used to combine the land cover data (ESA WorldCover 2021), hydrologic soil groups (HYSOGs), and look-up table to create a curve number map for the research area, which was subsequently incorporated into the SFINCS model. Like with the land cover map, the 10 m resolution of the data set is resampled to a 20 m resolution in the subgrid mode.

TABLE 3.2: Curve numbers for various land cover data sets and for different hydrologic soil groups. Adapted from: HEC-HMS (2023)

ESA Worldcover 2021	**NLCD 2019**	**HSG**			
Land cover	**Land cover**	**A**	**B**	**C**	**D**
80 - Permanent water bodies	11 - Open Water	98	98	98	98
50 - Built-up	21 - Developed, Open Space	49	69	79	84
	22 - Developed, Low Intensity	57	72	81	86
	23 - Developed, Medium Intensity	61	75	83	87
	24 - Developed, High Intensity	81	88	91	93
60 - Bare / sparse vegetation	31 - Barren Land (Rock/Sand/Clay)	78	86	91	93
10 - Tree cover	41 - Deciduous forest	45	66	77	83
	42 - Evergreen Forest	25	55	70	77
	43 - Mixed Forest	36	60	73	79
20 - Shrubland	52 - Shrub/Scrub	55	72	81	86
30 - Grassland	71 - Grassland/Herbaceous	50	69	79	84
	81 - Pasture/Hay	49	69	79	84
40 - Cropland	82 - Cultivated Crops	67	78	85	89
90 - Herbaceous wetland	90 - Woody Wetlands	30	58	71	78
	95 - Emergent Herbaceous Wetlands	30	58	71	78

3.2.1.4 Precipitation

The model was forced using gridded precipitation data. Two different forcing data sets were initially used in the model to analyse the differences in model results:

- **ERA5-Land**: ERA5-Land is the fifth generation reanalysis of global land variables from 1950 onwards (Muñoz-Sabater et al., 2021), developed by the ECMWF (European Centre for Medium-Range Weather Forecasts). It contains gridded climate data with a 0.1° x 0.1° spatial resolution (~9 km) and a 1-hour temporal resolution.
- **KNMI Reanalysis**: the KNMI Reanalysis was developed by the KNMI (Royal Dutch Meteorological Institute) for the event and it covers the 48 hours from July 13th 10:00 to July 15th 10:00 in 2021. It contains hourly data with a 100 x 100 m spatial resolution. It was created by combining rainfall measurements and radar measurements and should therefore more accurately represent the situation during the July 2021 event (Van Heeringen et al., 2022).

In the final model, the ERA5-Land data set was used (Fig. 3.4), despite the fact the KNMI Reanalysis is technically more accurate in terms of total precipitation. This choice will be discussed in more detail in Chapter 5.

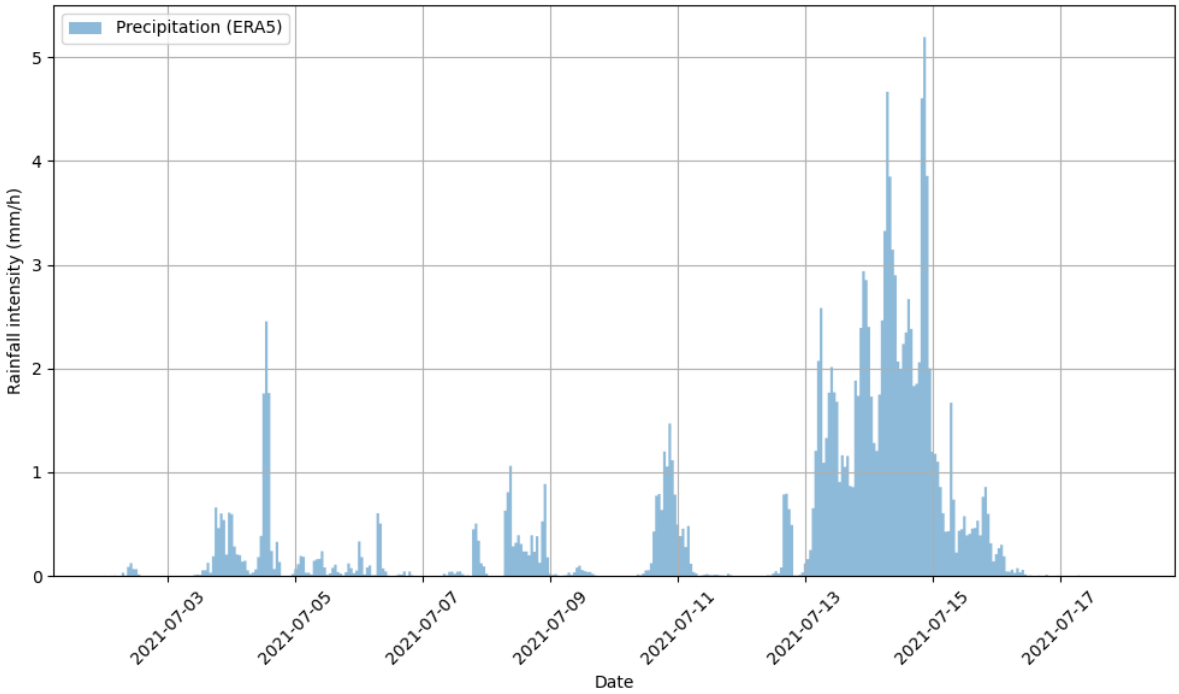

FIGURE 3.4: ERA5-Land rainfall intensity in the model period.

3.2.1.5 River centerlines and GloFAS

It is possible to 'burn' the river bathymetry into the subgrid to aid the routing of the water in subgrid mode. In the model for the Geul, the MERIT-Basins data set was used for the river centerlines. MERIT-Basins is a global vector hydrography database (P. Lin et al., 2019) derived from the 90-m MERIT-Hydro product (Yamazaki et al., 2019). To burn these centerlines into the subgrid, a width and depth must be assigned to the centerlines first.

According to Ahmed and Eslamian (2022), the bankfull discharge occurs, on average, every 1.5 years, but it may vary between a recurrence interval of 1 to 32 years. Based on the

bankfull discharge, the dimensions of a channel may be calculated. This requires discharge data for the stream at hand and for this research, the GloFAS-ERA5 data set was used. This is a global gridded dataset of river discharge with a horizontal resolution of 0.1° at a daily time step from 1979 until the present (Harrigan et al., 2020). This data set allows for the calculation of return periods using a generalized extreme value (GEV) distribution. From this GEV distribution, the discharge with a return of 2 years was selected (Sampson et al., 2015), which was then used to calculate the bankfull discharge. This discharge is then used to calculate the channel width using Equation 3.6, taken from Leopold and Maddock (1953). In this equation, w is the channel width, Q the discharge, and a and b numerical constants (7.2 and 0.5 respectively in this research). The calculated widths can then be used to estimate the depth (Sampson et al., 2015) using Manning's equation (Eq. 3.7). In this equation, Q is the discharge, A is the channel cross-sectional area, n is the Manning coefficient of roughness, R is the hydraulic radius (cross-sectional area divided by wetted perimeter), and S is the hydraulic gradient or channel slope. The calculated width and depth for each river section are then added to the MERIT-Basins centerlines and burnt into the subgrid.

$$w = aQ^b \tag{3.6}$$

$$Q = A \cdot \left(\frac{1}{n} R^{2/3} S^{1/2} \right) \tag{3.7}$$

3.3 Modelling afforestation effects

After a working model for the July 2021 event in the Geul has been created, various afforestation scenarios will be explored. This measure will be implemented by changing the input land cover maps and creating new curve number maps using the previously described method. Changing these input files will simulate the change in land cover type by changing the surface roughness and infiltration. Land cover and curve number maps for each scenario can be found in Appendix C and D respectively.

The implementation of nature-based solutions into hydrodynamic models is not common in this specific context. However, previous research has modelled an increase in green area by changing the land cover type, which then changes the underlying factors it influences, like the surface roughness, storage depth, infiltration rate, and runoff coefficient (E. Lin et al., 2016; Glenis et al., 2018; Lu and Sun, 2023). When it comes to using hydrodynamic models, the implementation of coastal vegetation is more common in literature. Such research often focuses on the implementation of mangroves, salt marsh vegetation, or seagrasses. They are usually implemented by changing vegetation parameters such as the stem diameter, stem height, vegetation density, drag coefficients, and frontal width (Niazi et al., 2021; van Zelst et al., 2021; Bennett et al., 2023; Chen et al., 2024). This level of detail in implementing vegetation is not possible in SFINCS, and therefore changing the surface roughness and curve numbers are the only two parameters that can represent the land cover change to forest cover. Curve numbers represent the land cover change to forest by reducing the fraction of the rainfall that turns into runoff. This represents the increased water loss to infiltration, interception, and evaporation. This method was chosen because it accounts for the intensity of the rainfall, as opposed to a flat infiltration rate. Another method that SFINCS can use is the Horton method (Leijnse, 2024), but the use of this method is not explored in this research. The Manning roughness increases when the land cover type is changed to tree cover. This means that water is slowed down more as it flows through the model domain, which could delay the peak discharge.

The sections below will discuss the various afforestation scenarios that will be implemented. Table 3.3 contains the tree cover and increase in tree cover in each scenario.

TABLE 3.3: Forest cover and increase in forest cover in the Geul catchment for each of the afforestation scenarios.

Scenario	**Fraction tree cover**	**Increase in tree cover**
Baseline scenario	30.3%	-
Full afforestation	92.7%	+62.4%
Upstream afforestation	56.9%	+26.7%
Downstream afforestation	66.0%	+35.7%
Policy scenario	31.1%	+0.8%
Riparian forests	38.4%	+8.2%
Hedges	34.7%	+4.4%

3.3.1 Full afforestation

In this scenario, the land cover in the entire Geul catchment will be converted to forest, except for the built-up area. This is a very unrealistic scenario, but it serves as an indication of the overall effect that afforestation can have. By exploring this scenario first, the maximum possible effectiveness of afforestation can be gauged first because previous research has suggested that afforestation can only have a limited effect on flood risk (Slager et al., 2022).

3.3.2 Upstream afforestation and downstream afforestation

These two scenarios are very similar to the first scenario, but in the upstream scenario, only the Belgian part of the catchment is converted to forest, and in the downstream scenario only the Dutch and German parts of the catchment are converted to forest. Like in the full afforestation scenario, the built-up area is left untouched during the conversion of the input maps. These scenarios serve to explore the difference between afforestation in the upstream and downstream parts of the catchment. Additionally, policy related to flood risk reduction often occurs on a national level, so these scenarios could show what is possible within the main countries in the Geul catchment.

3.3.3 Policy scenario

In reality, afforestation projects are often limited in size and extent. The province of Limburg in the Netherlands plans to expand the existing forest area in the province by 10% or 3,500 hectares by 2030 (Limburg, 2023). Accounting for the area of the Geul catchment located within the province of Limburg, this would amount to roughly 380 hectares of afforestation. Exact locations are not yet known for the forest expansion and therefore these 380 hectares of afforestation in Limburg have been selected at random. This should be taken into account when evaluating the results of this scenario. It is also not certain whether there will be 380 hectares of afforestation in the Geul catchment, this is based on an assumption. Instead, this scenario serves to see whether planned afforestation practices will already affect flood risk.

3.3.4 Riparian forests

Riparian buffer zones or forests serve a multitude of purposes. Most notably, they can store water and reduce floods, but they can also increase biodiversity, stabilize riverbanks, and improve water quality (Anderson, Masters, et al., 1992; Graziano et al., 2022). In this scenario, these zones are introduced by adding a buffer of 100 meters on both sides of the stream network in the entire catchment (excluding built-up area).

3.3.5 Hedges

Hedges or forest strips can act as infiltration zones by capturing and infiltrating water flowing on the surface of slopes. Hugtenburg et al. (2023) suggest implementing 10-20 meter wide infiltration zones parallel to elevation contour lines in cropland and grassland. For this research, 20-meter-wide hedges were implemented on grasslands throughout the Geul catchment. These hedges were implemented at a 15-meter elevation increment. Although this measure, like the policy scenario, does not add much forest area to the catchment, it might still have a delaying effect on the peak of the flow.

3.4 Different rainfall scenarios

The aforementioned scenarios will be run with the ERA5-Land data set for the precipitation forcing. In addition to these seven scenarios (the baseline scenario and six afforestation scenarios), the same scenarios will be run for different rainfall scenarios by changing the ERA5-Land forcing file. The additional rainfall scenarios are created by subtracting 20% and 50% from the rainfall in the ERA5-Land data set. This creates less extreme rainfall scenarios to assess the effects of afforestation. This choice was made because research suggests that factors like land cover do not influence the runoff as significantly during extreme rainfall events (Johnen et al., 2020; Cheng et al., 2021; Manes et al., 2024). The final model scenarios are displayed in Table 3.4.

TABLE 3.4: The different model scenarios in this research.

Run number	ERA5	ERA5-20%	ERA5-50%
1, 2, 3	Baseline scenario	Baseline scenario	Baseline scenario
4, 5, 6	Full afforestation	Full afforestation	Full afforestation
7, 8, 9	Upstream afforestation	Upstream afforestation	Upstream afforestation
10, 11, 12	Downstream afforestation	Downstream afforestation	Downstream afforestation
13, 14, 15	Policy scenario	Policy scenario	Policy scenario
16, 17, 18	Riparian forests	Riparian forests	Riparian forests
19, 20, 21	Hedges	Hedges	Hedges

3.5 Validation of model performance

The performance of the model for the July 2021 event will be validated before implementing the various afforestation scenarios. This evaluation is done by comparing the observed flood extent (Slager et al., 2021) with the modelled flood extent in SFINCS. This evaluation is done in a validation region within the Geul catchment that was created by creating a 100-meter buffer around part of the observed flood extent (Fig. 3.5). It should be noted that the data set by Slager et al. (2021) might not be fully accurate in displaying the maximum flood extent either, which should be considered when evaluating the model performance using this data set.

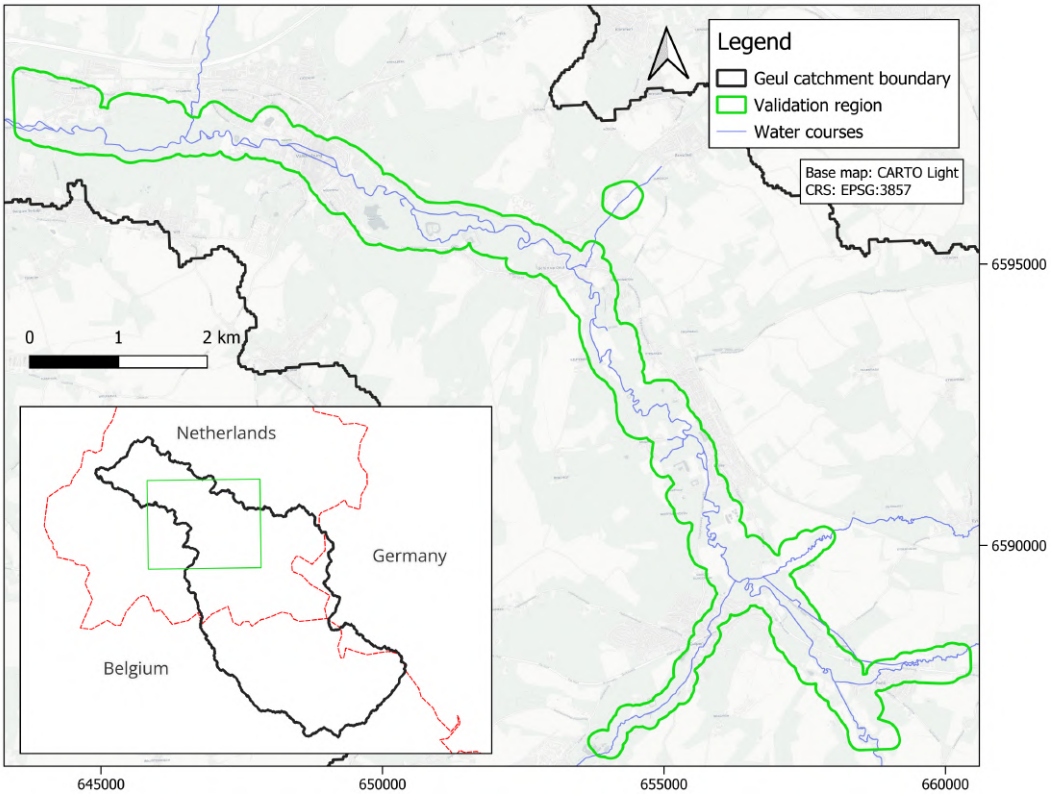

FIGURE 3.5: The validation region in which the performance metrics are calculated.

The performance itself is quantified by calculating various performance metrics within the validation region (Sampson et al., 2015; Oruc Baci et al., 2024) :

- **Hit rate (H)**: this metric calculates the ratio between the overlap of the observed and simulated flood extent (B) and the total observed flood extent ($A \cup B$). This metric varies between 0 (no observed flood accurately predicted) and 1 (all observed flood accurately predicted). It is only able to detect an underestimation in the modelled flood extent.

$$H = \frac{B}{A \cup B} \tag{3.8}$$

- **False alarm rate (F)**: this metric calculates the ratio between the modelled flood extent outside the observed flood extent (C) and the total modelled flood extent ($B \cup C$). This metric varies between 0 (no false alarms) and 1 (all false alarms). It is only able to detect overestimation in the modelled flood extent; the higher the value, the more overestimation in the modelled flood extent.

$$F = \frac{C}{B \cup C} \tag{3.9}$$

- **Critical Succes Index (CSI)**: this metric calculates the ratio between the overlap of the observed and simulated flood extent (B) and the total flooded area obtained in both the model and the observations ($A \cup B \cup C$). It varies between 0 (no correlation between modelled and observed flood extent) and 1 (perfect match between model and observations).

$$CSI = \frac{B}{A \cup B \cup C} \tag{3.10}$$

- **Error bias (E)**: this metric gives information about the tendency of the model to overestimate or underestimate the flood extent. It is the fraction between flood extent only in the observations (A) and the flood extent only in the model (C). If $E = 1$, there is no bias; if $E > 1$, there is an overestimation; if $E < 1$, there is an underestimation.

$$E = \frac{C}{A} \tag{3.11}$$

Additionally, the observed water levels at Meerssen and the observed discharge at Sippenaeken will be compared to the modelled water levels and discharge at these locations (Fig. 2.1). This should provide more insight into the model behaviour. It should be noted that the discharge and water levels at specific locations are not a primary output of the SFINCS model because it was primarily developed as a flood model. Therefore, these metrics might not be as accurate as in other models.

3.6 Analysis of afforestation effects

After the evaluation of the model performance, this model will be used as a baseline to analyse the effects of the various afforestation scenarios. After implementing a new forest scenario, the discharge at Meerssen in the baseline scenario will be compared to the discharge in the new scenarios. The effects on the peak discharge (expected reduction) and the timing of the peak (expected delay) will be assessed. A similar approach will be taken when looking at the modelled total flood extent. By comparing the baseline scenario with the afforestation scenarios (expected decrease in flood extent), their effectiveness will be assessed.

Chapter 4

Results

4.1 Model performance

This section will discuss the model performance by calculating the previously described performance metrics on flood extent. Additionally, the observed water levels at Meerssen and the discharge at Sippenaeken will be compared to their simulated counterparts.

4.1.1 Flood extent

Figure 4.1 shows the observed flood extent and modelled flood extent in the validation region. As shown in the figure, the model tends to underestimate the flooded area in parts of the validation region, especially around parts of the main channel. This is confirmed by the performance metrics (displayed in Fig. 4.1); the error bias of 0.61 and hit rate of 0.80 indicate an underestimation of the observed flood extent in the model. Conversely, the false alarm rate of 0.14 indicates that there is little overestimation in the model. A CSI of 0.85 hints at a generally good performance of the model in matching the observed flood extent (Hocini et al., 2021).

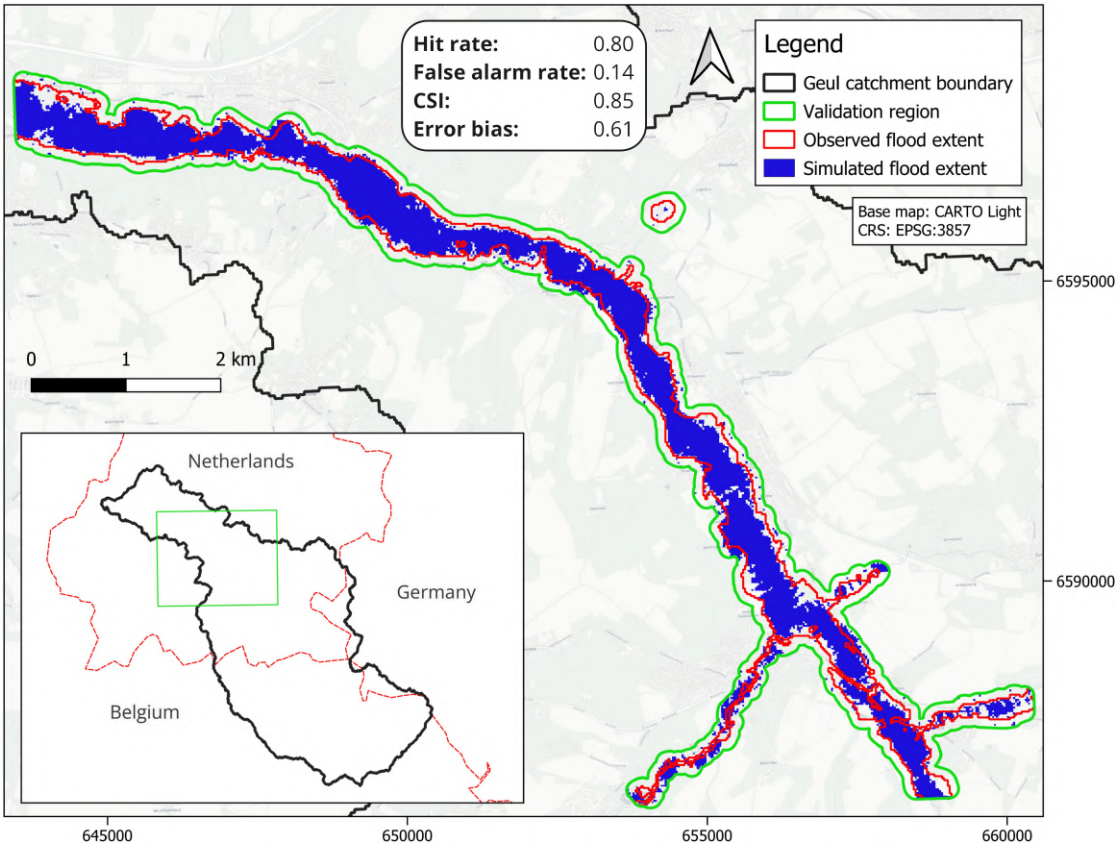

FIGURE 4.1: The observed and simulated flood extent.

4.1.2 Discharge

Figure 4.2 shows the modelled and observed discharge at Sippenaeken in the period 02-07-2021 to 18-07-2021. The figure shows that the model performs poorly at displaying the base flow. Instead, the discharge remains mostly 0 m^3/s until the very intense rainfall event around 13-15 July. This might be a result of the fact that SFINCS does not start with a base flow but instead starts with a completely dry catchment.

The peak event of the event also looks very different from the observations. The rising limb occurs around the same time, but the falling limb occurs sooner (the model returns to baseflow much more quickly). The peak of the discharge is also much higher than expected at 82.9 m^3/s. This is closer to the estimated discharge at Meerssen of 87.5 m^3/s, which is much further downstream (Van der Veen & Agtersloot, 2021).

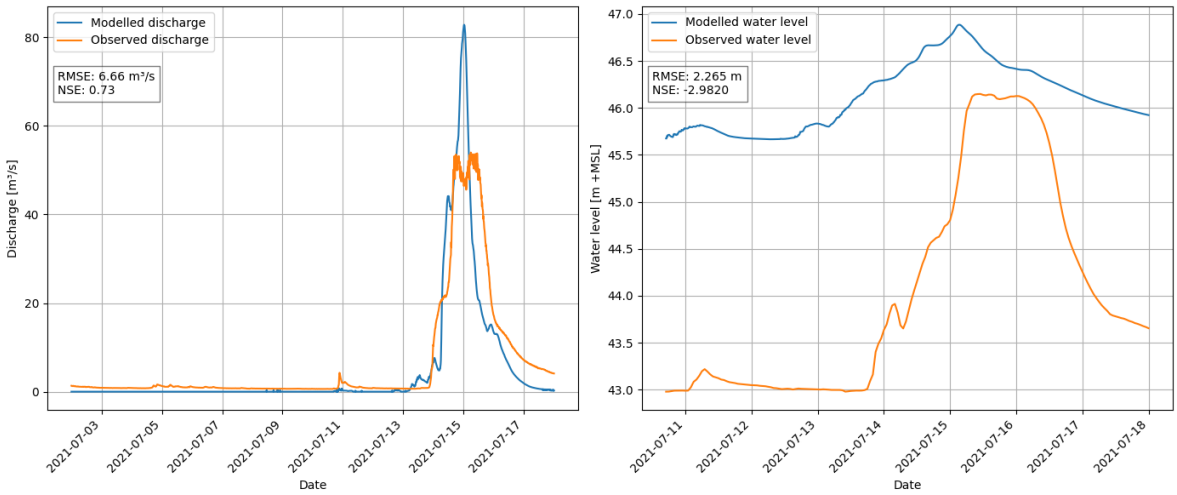

FIGURE 4.2: Observed and modelled discharge at Sippenaeken (left) and observed and modelled water levels at Meerssen (right).

4.1.3 Water levels

As seen in Figure 4.2, there is a large discrepancy between the observed and modelled water level at Meerssen in the period, with poor performance regarding the RMSE and NSE as a result. This discrepancy is likely caused by a difference in elevation between the model and reality in this location. The river depth calculated using the method from Leopold and Maddock (1953) is only 0.45 m, which is burned into the DEM. However, high-resolution elevation data (AHN, 2024) shows that the river bank is over two meters deep in this location. This means that the model setup underestimates the bed elevation of the river significantly in this location: the bed elevation in the model is 45.62 m, whereas the bed elevation in reality is at least 43.17 m. This difference explains the discrepancy between the modelled and observed water levels. The shape of the figure is also different. For example, the increase in water level is not as significant, which is likely caused by the river overflowing into the floodplain more quickly in the model. The water level also starts to rise more quickly than in the observations, which suggests that the water is routed through the catchment more quickly in the model than in reality.

4.2 Afforestation effects

This section presents the results of the different afforestation scenarios and rainfall scenarios. The first part will focus on the modelled peak discharge at Meerssen and how it changes under different afforestation and precipitation scenarios. The second part will focus on the total modelled flood extent in the catchment and how it changes under those same scenarios.

4.2.1 Discharge at Meerssen

In Figure 4.3 the discharge for each of the afforestation scenarios is plotted, along with the percentage of decrease from the baseline scenario. Note that the SFINCS model grossly overestimates the discharge at Meerssen as well, with a peak discharge of 195.5 m^3/s at Meerssen. This is much higher than the estimated peak discharge of 87.5 m^3/s in Van der Veen and Agtersloot (2021).

In terms of afforestation effects, the reduction in peak discharge is largely proportional to the amount of forested area that is added in each scenario. In the full afforestation scenario, the reduction in peak discharge is 32.7%. This is a significant effect and it shows that increasing the forest cover can have an influence on the discharge. For the scenarios that add less forest to the catchment, the discharge reduction is lower. This can be seen in the upstream, downstream, and riparian forests scenarios. However, riparian forests have a more significant effect on discharge when compared to the forest area it adds to the catchment. It adds 8.2% forest cover, compared to the 26.7% and 35.7% increase in the upstream and downstream scenario respectively, but its effect on the peak discharge is roughly similar in the ERA5 and ERA-20% precipitation scenarios. The policy scenario and the hedges scenario have a very limited effect on the peak discharge (-0.7% to -2.6%), which is likely the result of the limited increase in forest cover in these scenarios.

In the different precipitation scenarios, the signal is mostly similar for the different afforestation scenarios. The relative effect on discharge reduction is more significant for the lighter ERA5-20% scenario, which hints at a greater sponge effect under these lighter rainfall conditions. For the ERA-50% scenario, the signal is slightly different. Here, the effect of downstream afforestation (-45.6%) is closer to that of full afforestation (-52.5%), and the effect of upstream afforestation is much more limited (-7.0%). The more realistic policy and hedges scenarios have a more significant, but still limited, effect under these lighter rainfall conditions. Discharge plots for each precipitation scenario can be found in Appendix E.

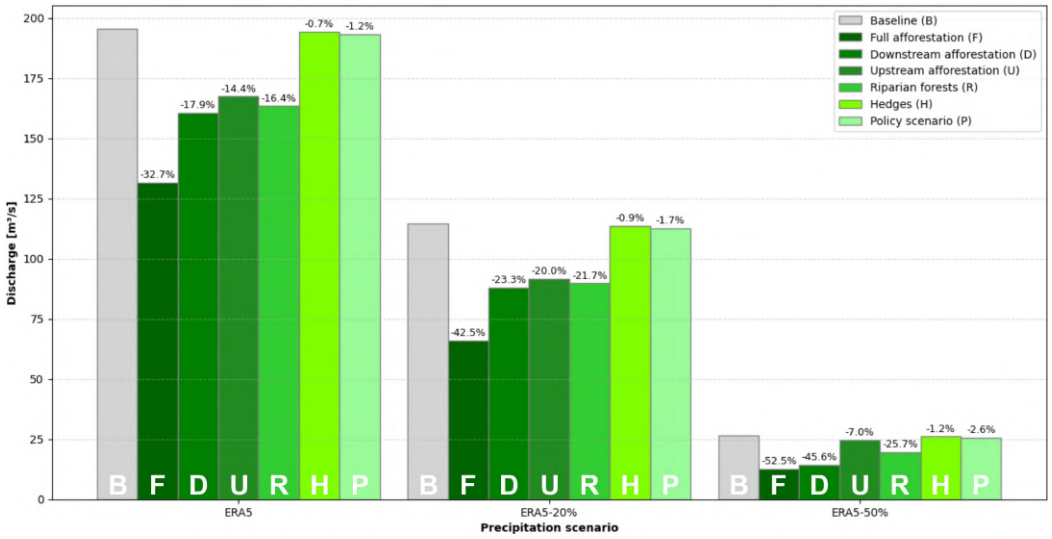

FIGURE 4.3: Peak discharge at Meerssen in each of the model scenarios.

Table 4.1 shows the timing of the discharge peak for each of the scenarios. For almost every scenario, the increase in forest cover leads to a delay in the peak discharge. Note that the SFINCS output is in increments of 10 minutes, so changes smaller than this increment cannot be observed in these results. The results seem to indicate that a higher increase in forest cover also leads to a greater increase in lag time. The high forest cover in the more extreme afforestation scenarios results in the water being slowed down more as it flows through the catchment. However, this is not true for the upstream afforestation scenario. This indicates that the location of afforestation plays a big role as well. The riparian forests scenario suggests this as well, with it having a significant effect in delaying the peak, despite the more limited extent of afforestation. The table also shows that hedges delay the peak by less than 10 minutes in the ERA5 precipitation scenario, whereas it does show a delaying effect in the lighter rainfall scenarios. This could suggest that this measure is more effective during less extreme rainfall scenarios.

TABLE 4.1: Time of peak discharge in the baseline scenario for each precipitation scenario and the respective delay for each afforestation scenario.

	ERA5	**ERA5-20%**	**ERA5-50%**
Baseline	15-7-2021 03:00	15-7-2021 04:10	15-7-2021 07:10
Full afforestation	+04:30	+07:30	+10:20
Upstream afforestation	+00:20	+00:40	+00:00
Downstream afforestation	+04:00	+05:00	+10:00
Policy scenario	+00:20	+00:20	+00:40
Riparian forests	+02:40	+03:40	+05:00
Hedges	+00:00	+00:10	+00:10

4.2.2 Flood extent

Figure 4.1 shows the total flood extent in the Geul catchment for all the different scenarios. Note that cells only count as flooded in the model when the water depth exceeds 0.05 meters. This means that changing this threshold would influence the modelled flood extent. Overall, the change in modelled flood extent is not in line with expectations.

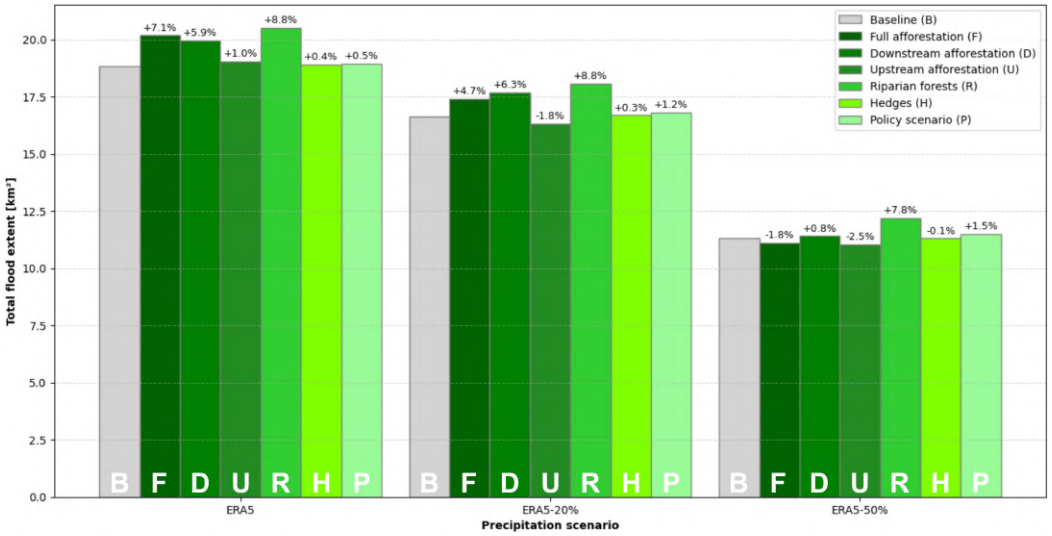

FIGURE 4.4: Total flood extent in the Geul catchment for each scenario.

As previously discussed, an increase in forest cover should lead to more infiltration, thus reducing the flooded area. However, the model results show an increase in flood extent in almost every scenario. Most notably, the riparian forest scenario shows the largest increase in each of the precipitation scenarios (+7.8% to +8.8%). A decrease in flood extent only occurs for some of the afforestation scenarios in the less extreme rainfall scenarios. Even then, the reductions in flood extent are not large (-0.1% to -2.5%). The explanation for this outcome can be found in a combination of two factors. These factors are the way infiltration is implemented into the model and the way the channel dimensions are calculated. This will be discussed in more detail in Chapter 5.

Chapter 5

Discussion

5.1 Model input and setup

Various choices were made for the input files. The resolution of the DEM and other input files can influence the output, but this is also largely dependent on the subgrid settings. In the current setup, the flux calculations were calculated on a 100-meter grid and then overlain on a 20-meter subgrid. Changing these settings (subgrid size and number of subgrid cells) influences the model output. Different combinations were tried for the model but the current combination proved effective in terms of model results and computation time.

An unexpected result was found when changing the model period. When the model was run between 11-7-2021 and 18-7-2021 instead of 2-7-2021 to 18-7-2021, the model severely underestimated the discharge at Meerssen. Changing the starting date only removes some relatively minor rainfall events, but the longer period leading up to the large event around 13-15 July acts as a spin-up period for the model. This is especially important because the model starts with a catchment that is essentially devoid of water at the start of the modelled period. It is important to keep this in mind when analysing the results or when setting up a model for a similar situation where precipitation is the only type of forcing. No previous research has used SFINCS for a headwater catchment like this, so it is unknown if this corresponds with other research. Instead, rivers are often forced with discharge or water level time series (Nederhoff et al., 2024) or reservoir releases (Sebastian et al., 2021).

5.1.1 Forcing data

The choice of forcing data also proved to have a significant influence on the results. The KNMI Reanalysis should provide a more accurate representation of the rainfall in the model domain during the July 2021 event. However, using this data set led to an even larger overestimation of discharge than is already the case. At Meerssen, the modelled peak discharge was over 250 m^3/s; more than three times the estimated discharge by Van der Veen and Agtersloot (2021). Because of this, the choice was made to use the ERA5-Land data set, which results in lower peak discharges. The cause for this overestimation (which is still present when using ERA5-Land) is likely an underestimation of certain processes in SFINCS. For example, infiltration and evaporation are only implicitly represented through the curve number method, but using this method leads to an overestimation of the runoff. Which could suggest that some of these processes might be underestimated. The drawbacks of using this method will be discussed in more detail later in this chapter. The model also does not include a groundwater component, which might influence the model results over longer periods. Having a groundwater flow or storage component can result in a more accurate representation of the baseflow through the slow release of water from the ground to the streams (like in the Geul catchment with the chalk and limestone aquifers).

5.1.2 Calculating channel dimensions

The previous chapter already discussed the observed gap in the observed and modelled water levels at Meerssen. The calculated channel bed elevation of 45.62 m is much higher than the observed bed elevation of at least 43.17 m. This leads to problems when measuring the water levels but it can also cause the channel to overflow more quickly in the model than in reality. This is partially compensated by the fact that the calculated river width tends to overestimate the actual river width: the observed channel width near Meerssen is around 10-12 m but the calculated width using Leopold and Maddock (1953) is 21 m. This still leads to an underestimation of the channel cross-sectional area, causing it to overflow more quickly in the model. This would not influence the results much when modelling extreme events, but it does lead to additional uncertainties when modelling the lighter precipitation events.

Further research could focus on improving the estimations of channel dimensions for this catchment. This can be done by changing the numerical parameters in Equation 3.6 or by increasing the return period of the discharge that is used to calculate the channel dimensions. Alternatively, measurements of the channel dimensions for the Geul could be added to the model. This might improve results for the Geul but it makes the workflow less applicable to other catchments, especially in catchments where measurements of channel dimensions are not available.

5.1.3 Manning values and curve numbers

The land cover dictates the Manning roughness and curve numbers in the model. Literature shows a broad range in Manning values for different land cover types (Kalyanapu et al., 2009; Nyaupane et al., 2018). Investigating the sensitivity of the model to the Manning roughness for different land cover types could be interesting in further research. For the curve numbers, this would be even more important because the model currently overestimates the total runoff. Previous research has shown that changes of 15-20% in the curve numbers can double or half the total estimated runoff (Boughton, 1989). Ponce and Hawkins (1996) also suggest the method's sensitivity to the curve number as a potential disadvantage, as well as its varying accuracy in different biomes. They also mention the lack of clear guidance on determining the antecedent moisture conditions, which is also a major influence on the curve numbers. The variation in curve number values might not play a large role during more extreme rainfall events, as suggested by Bondelid et al. (1982). They note that the effects of curve number variation on estimated runoff decrease for larger storm events. This could suggest that varying the curve numbers could play a significant role in the less extreme ERA5-20% and ERA5-50% rainfall scenarios. The use of curve numbers for this type of research will be discussed in more detail later in this chapter.

5.2 Model validation

The model for the July 2021 event in the Geul performed well when looking at flood extent as a proxy for model performance. The CSI of 0.85 indicates that the flood extent could be simulated with the model fairly well, although there was an underestimation of the observed flood extent. As mentioned in Chapter 4, there is also an uncertainty in the observed flood extent, which is why a decision was made to look at a validation region within this data set instead of at the whole catchment.

Because of the uncertainty in the observed flood extent, the modelled discharge at Sippenaeken and modelled water levels at Meerssen were also compared to their observed counterparts. For the water levels at Meerssen, a gap of roughly 2.7 m was found between

the modelled and observed water levels. This gap likely is caused by the low resolution of the DEM combined with the significant underestimation of the river depth from using the Leopold and Maddock method. Subtracting 2.7 m from the modelled water levels brings it closer to the observed water levels but the modelled peak is still a very poor fit (Fig. 5.1), which is also suggested by the Nash-Sutcliffe efficiency of 0.11 of this corrected water level.

This is similar to the results for modelled discharge at Sippenaeken. The model does not manage to capture the finer details or dynamics in water levels and discharge. One explanation for this might be the fact that modelling discharge and water levels in small inland catchments like the Geul is not what SFINCS was originally developed for.

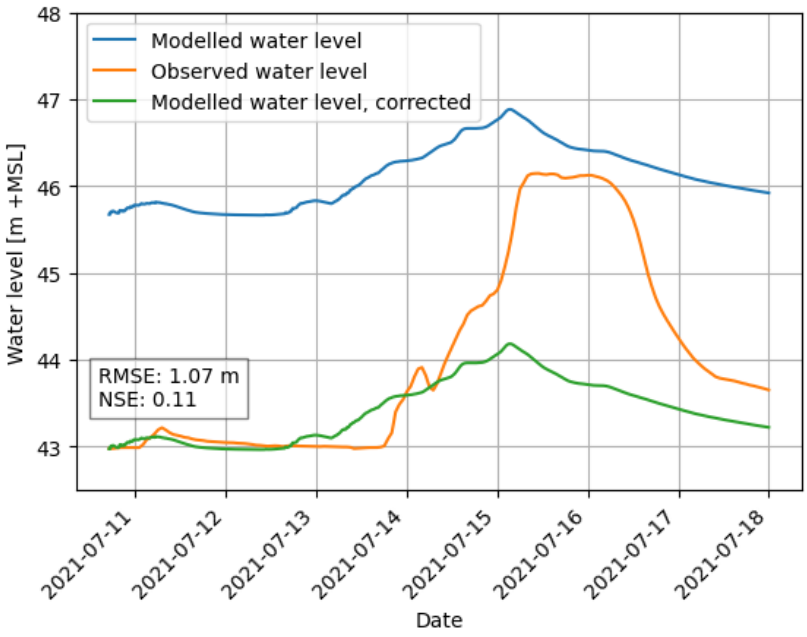

FIGURE 5.1: Modelled and observed water levels at Meerssen including the corrected modelled water level.

5.3 Afforestation results

The goal of this research was to investigate the implementation of nature-based solutions in the form of afforestation scenarios into the SFINCS model. The results show some expected outcomes (decreased peak discharge) but also some unexpected results (increased flood extent). This section will discuss these results and attempts to explain why they might not be in line with expectations.

5.3.1 Effects on discharge

A reduction in discharge was modelled for each of the afforestation scenarios (Table 5.1). Generally, we can see a higher reduction in peak discharge when more forest area is added. A notable exception is the riparian forests scenario, which results in a greater reduction in peak discharge than the upstream afforestation scenario, despite adding less forest area. The policy scenario is also more effective at reducing peak discharge than hedges, even though the hedges scenario adds more forest area to the catchment. This suggests that the spatial distribution of the afforestation also influences its effectiveness. However, it must be noted

that the spatial distribution of the rainfall can also influence these results. If more rainfall occurs over forested areas in the model, less runoff will be generated.

The timing of the peak discharge as presented in the previous chapter suggests that small increases in forest cover can already result in a delayed discharge peak in light rainfall scenarios. In the policy scenario, a 20-minute (ERA5) to 40-minute (ERA5-50%) delay was modelled in the peak discharge. These relatively small delays can already be significant during extreme events. In combination with good early warning systems, these delays can allow for more preparation or evacuation time, which could reduce economic damages or even save lives (Najafi et al., 2024).

TABLE 5.1: Reduction in peak discharge in each scenario. The afforestation scenarios are sorted from highest to lowest amount of forest area added.

	ERA5	**ERA5-20%**	**ERA5-50%**
Full afforestation	-32.7%	-42.5%	-52.2%
Downstream afforestation	-17.9%	-23.3%	-45.6%
Upstream afforestation	-14.4%	-20.0%	-7.0%
Riparian forests	-16.4%	-21.7%	-25.7%
Hedges	-0.7%	-0.9%	-1.2%
Policy scenario	-1.2%	-1.7%	-2.6%

5.3.2 Effects on flood extent

The modelled flood extent shows the most unexpected results. For nearly all scenarios, an increase in flood extent was modelled (Table 5.2). This highlights one of the underlying problems with the way the model was set up. The main reason for this is the use of the curve number method to determine infiltration. The curve number estimates the runoff directly from the precipitation falling on a cell. This means that there is no way for water to infiltrate when it is flowing through the catchment afterwards. This is not a problem when it comes to discharge because the discharge shows a clear signal when more forest is added (reduction in peak discharge), but it becomes more complicated when looking at the flood extent. When there is a lot of forested area in a floodplain, there is generally more infiltration, thus reducing the flood extent when the river overflows into the floodplain. This process does not happen in the SFINCS when the curve number method is used. Therefore, slowing down the water is the only effect the forest cover has in this case (higher Manning roughness coefficient). The slowing down of the water means that the water is routed out of the catchment less quickly, which means that the water flows into the floodplain further. This comes back in the model output as an increase in the flood extent for scenarios with more forest cover.

TABLE 5.2: Change in flood extent for each scenario. The afforestation scenarios are sorted from highest to lowest amount of forest area added.

	ERA5	**ERA5-20%**	**ERA5-50%**
Full afforestation	+7.1%	+4.7%	-1.7%
Downstream afforestation	+5.9%	+6.3%	+0.8%
Upstream afforestation	+1.0%	-1.8%	-2.5%
Riparian forests	+8.8%	+8.8%	+7.8%
Hedges	+0.4%	+0.3%	-0.1%
Policy scenario	+0.5%	+1.1%	+1.5%

Overall, this suggests that the curve number method is not the best choice when trying to model the effects of NBS/afforestation on flood extent. It can be effectively used to model the effect of afforestation on discharge (Waterloo & Gevaert, 2023), but when investigating where the water is going spatially it is not the best choice.

5.4 Using SFINCS for research on NBS

The results suggest that SFINCS can be used to model the effects of afforestation when looking at discharge to assess its effectiveness. However, the major flaws with the curve number method mean that measuring its effect on flood extent is not possible. Several alternative options exist for incorporating infiltration into SFINCS, such as a spatially varying flat infiltration rate and the Horton method (Leijnse, 2024). Further research could investigate how these methods perform when investigating the effects of land cover changes on flood extent. However, SFINCS lacks a certain complexity that can be incorporated into other (hydrologic) models. For example, the model essentially starts with a dry catchment, which means it needs a "spin-up" period when running it for research like this, but research would need to be carried out first to determine the minimum required spin-up time. Additionally, other models can often incorporate more information about the subsurface (soil, geology, groundwater, organic matter content) or information about the vegetation (bulk density, canopy cover, transpiration). Some of these factors make these models more fit for investigating nature-based solutions and their hydrological effects because it allows for much more freedom when incorporating (different types) of nature-based solutions into the model.

For a more complete understanding of the effects of nature-based solutions, research would also need to be done on the effect of these measures during dry periods. This is not directly possible in SFINCS because this is beyond the purpose of what the model was developed for. This makes hydrologic or combined hydrologic-hydrodynamic models a better choice because they can more effectively paint a complete picture of the effects of nature-based solutions.

Chapter 6

Conclusions

This research has shown that it is possible to reproduce the July 2021 floods in SFINCS quite well with a CSI of 0.85. One of the great strengths of the model is the subgrid mode, which allowed the model to run fast while still producing accurate results. This has shown that SFINCS can be effectively used in small inland river catchments, despite the model being originally developed for coastal compound flooding. Further research might reach even better results, for example by using more realistic channel dimensions. Exploring the use of different infiltration methods and Manning roughness coefficients would also be an interesting topic for further research. The infiltration (method) and the choice of precipitation forcing require more research, especially because the model still overestimates the discharge significantly in the current setup (by around 120% near the outlet of the catchment).

Problems arise when trying to apply to the model to researching the effects of afforestation in the catchment. These land cover changes are implemented through changes in the Manning roughness coefficients and curve numbers (which determine the runoff based on the precipitation intensity). These land cover changes result in a reduction in peak discharge that is mostly proportional to the amount of forest area that is added. However, the modelled flood extent consistently increases when more forest area is added. This is caused by the fact that the use of the curve number method does not allow for infiltration of water after the curve number calculation has been performed. This means that more forest area in the floodplains does not lead to more infiltration when the river overflows from the channel onto the floodplain. Instead, the water is only slowed down, resulting in a larger flood extent.

Further research can be done using the SFINCS model by, for example, testing different infiltration methods. However, for a more complete understanding of the effects of nature-based solutions, other models might be a better choice. Models that can accurately model evaporation/transpiration have an edge in this type of research (SFINCS does not contain a way to implement evaporation at all, instead it is only implicitly included in the curve number method). Being able to model both types of weather extremes (floods and droughts) is important when assessing the effects of nature-based solutions. This is necessary because policymakers need to know the full effect of implementing measures like these. If this is not known, unexpected negative effects can arise after measures have already been implemented.

To conclude, SFINCS has proven to be a useful tool in modelling the flood extent in small river catchments like the Geul at a fraction of the computational time that other models might require. However, it has proven to be a poor model choice when it comes to assessing the effects of nature-based solutions.

Appendix A

Software, hardware, and run times

A.1 Used software and hardware

Used desktop for all processes was a single 8 GB RAM, 2 cores, 4 logical processors, 2.50 GHz, Intel(R) Core(TM) i5-7200U CPU. For SFINCS, the SFINCS v2.0.3 Cauberg release was used. Model runs were performed using HydroMT-SFINCS in Visual Studio Code (v1.90.2). In Visual Studio Code, Python v3.10.13 was used with the Miniforge3 installer. For QGIS, the QGIS 3.34.3 Prizren release was used.

A.2 Model run times

TABLE A.1: SFINCS run time in minutes and seconds for each model scenario.

	ERA5	**ERA5-20%**	**ERA5-50%**
Baseline	21m42s	18m06s	13m17s
Full afforestation	17m45s	16m13s	14m43s
Downstream afforestation	19m24s	17m32s	14m23s
Upstream afforestation	19m32s	17m35s	14m42s
Riparian forests	17m59s	15m24s	12m39s
Hedges	17m36s	15m32s	11m28s
Policy scenario	18m43s	15m40s	13m34s
Average	**18m57s**	**16m35s**	**13m32s**

Appendix B

Geology and land cover

B.1 Geology

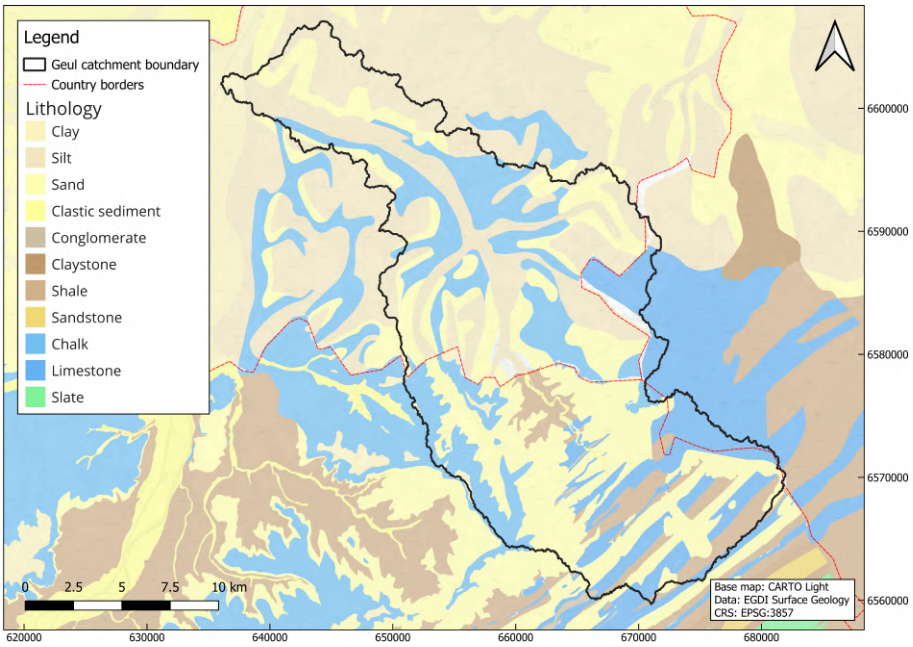

FIGURE B.1: Map of the surface geology/lithology in the region. Data from: EGDI (2016).

B.2 Land cover

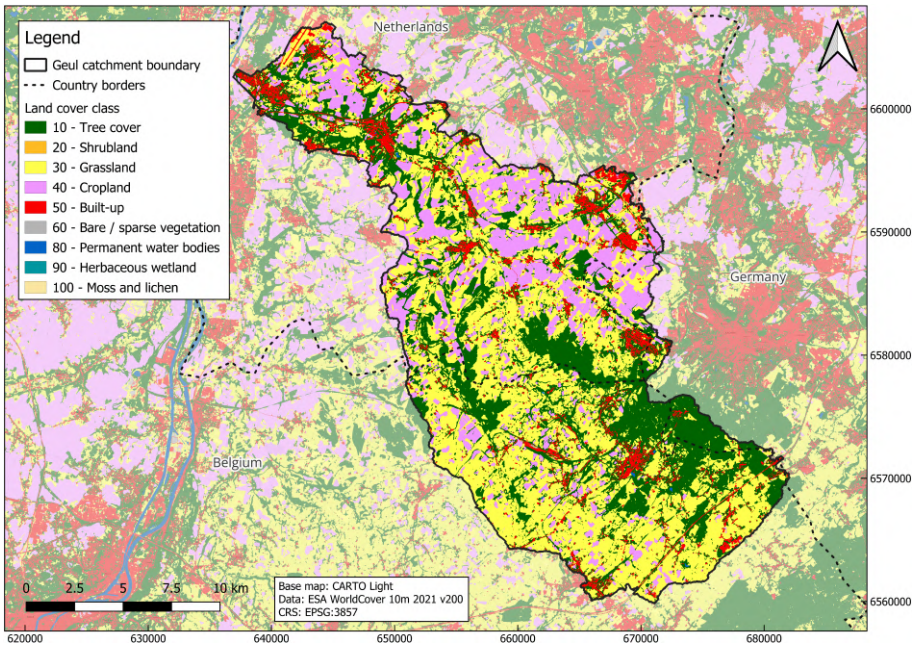

FIGURE B.2: Map of the land cover in the region. Data from: Zanaga et al. (2022).

Appendix C

Land cover maps

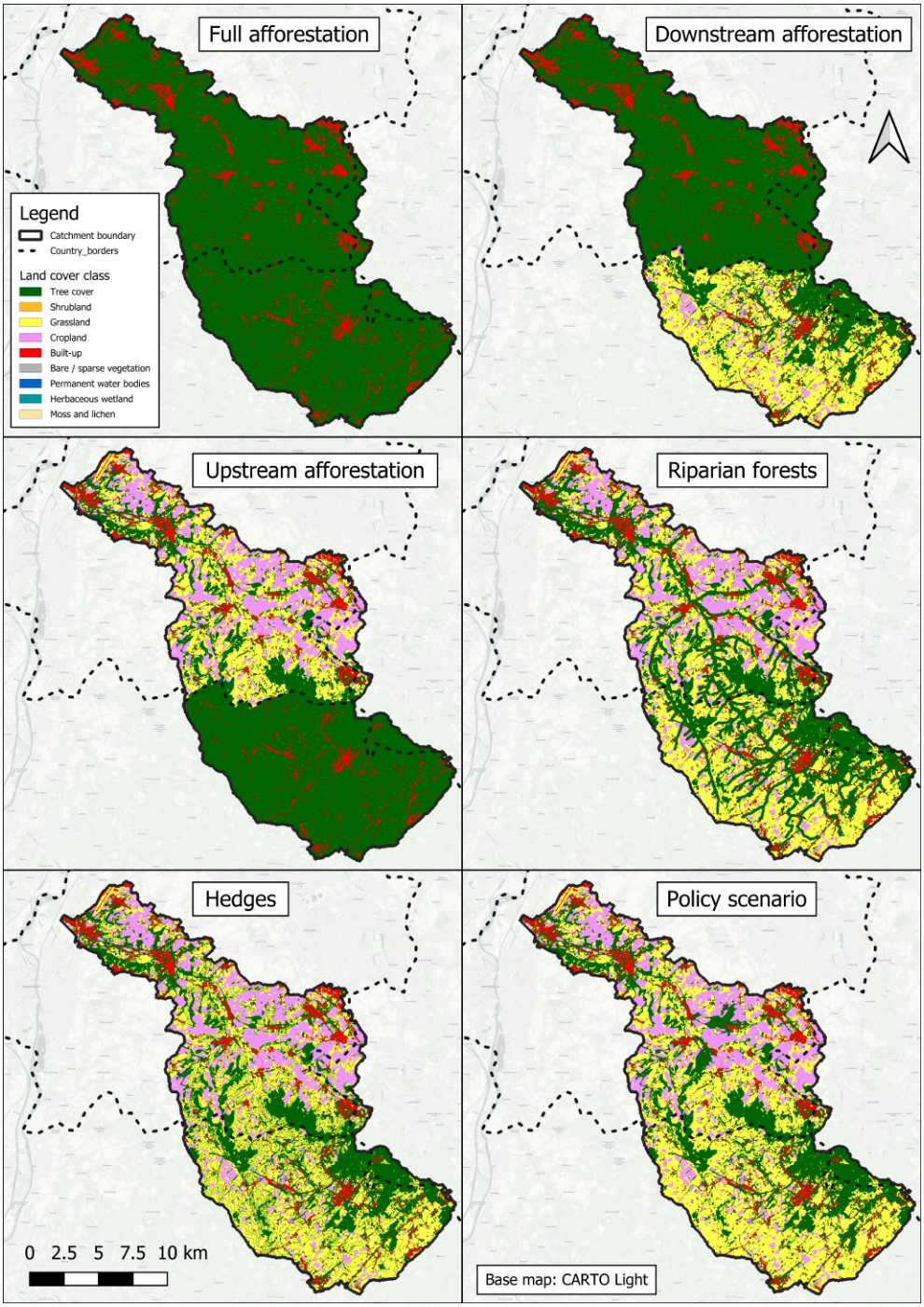

FIGURE C.1: Map of the land cover for each of the afforestation scenarios.

Appendix D

Curve number maps

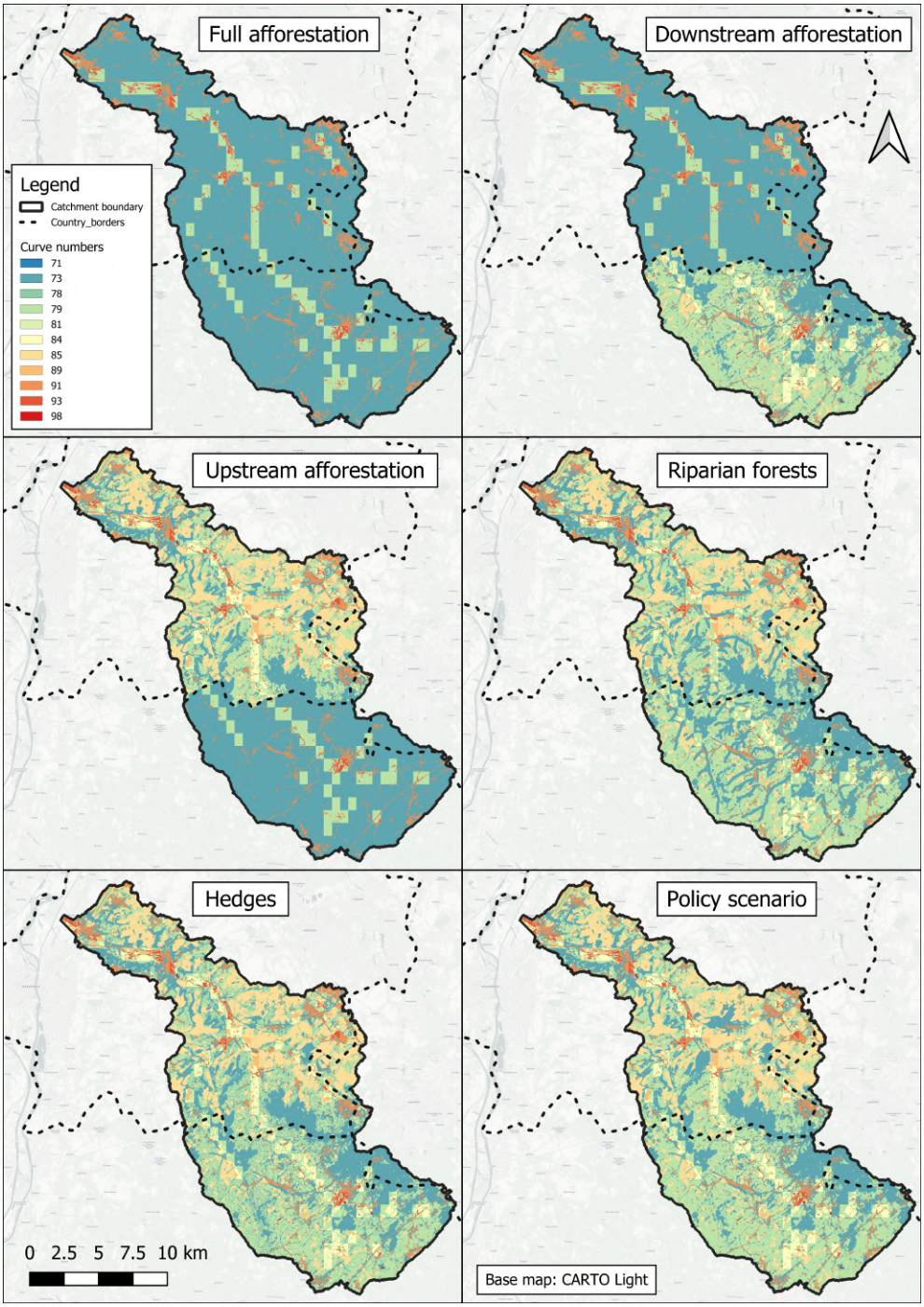

FIGURE D.1: Map of the curve numbers for each of the afforestation scenarios.

Appendix E

Discharge plots

E.1 Forcing: ERA5

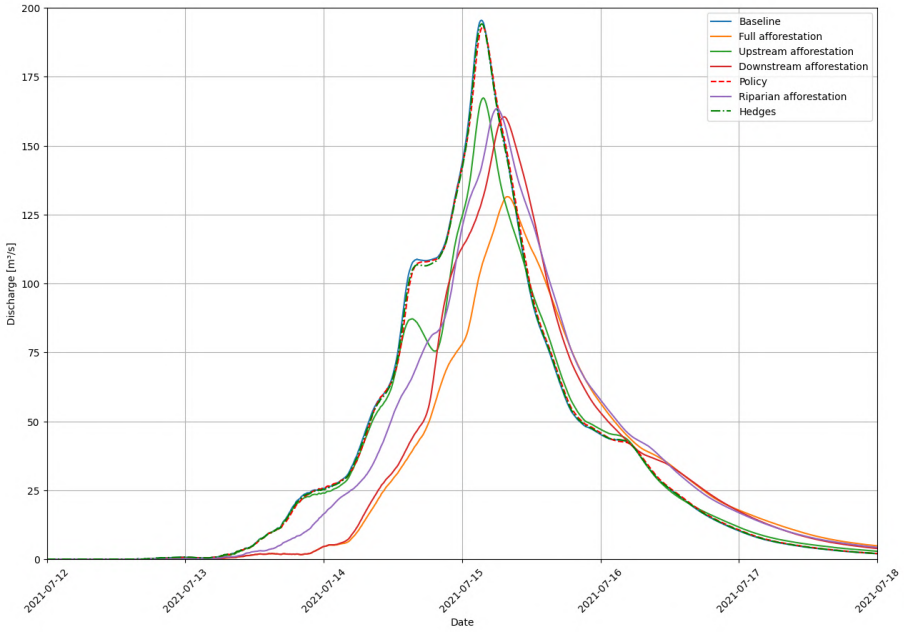

FIGURE E.1: Discharge for each afforestation scenario with the ERA5 forcing.

E.2 Forcing: ERA5-20%

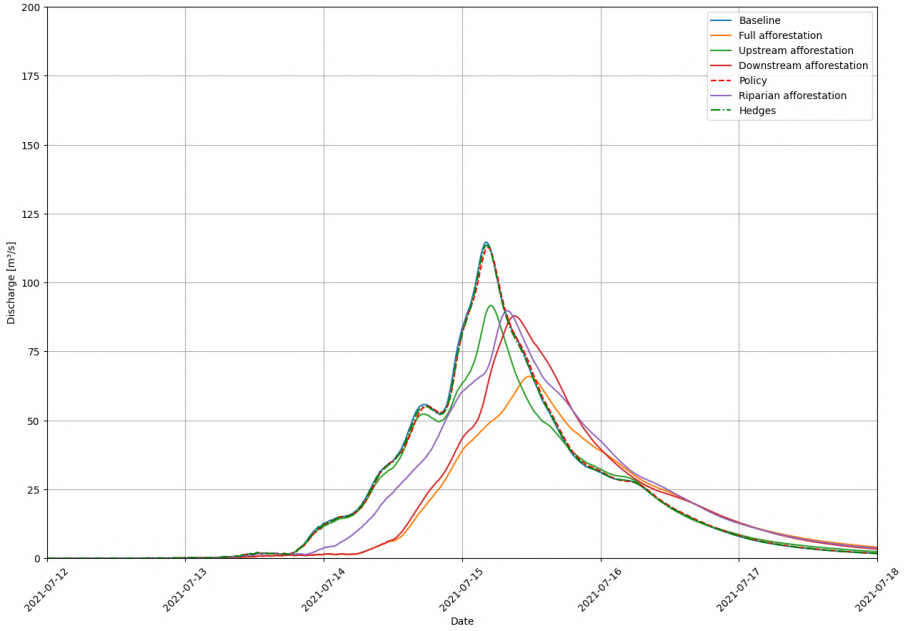

FIGURE E.2: Discharge for each afforestation scenario with the ERA5-20% forcing.

E.3 Forcing: ERA5-50%

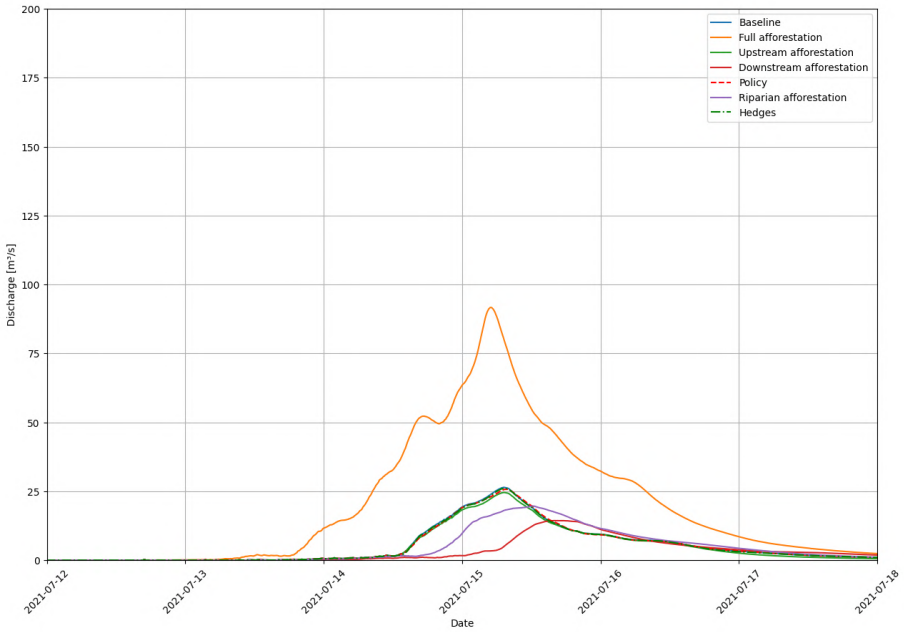

FIGURE E.3: Discharge for each afforestation scenario with the ERA5-50% forcing.

Bibliography

Ahmed, I., & Eslamian, S. (2022). Bankfull stage and flood return periods. In *Flood handbook*. CRC Press. https://doi.org/10.1201/9781003262640

AHN. (2024). Actueel hoogtebestand nederland - ahn4. https://ahn.arcgisonline.nl/ahnviewer/

Anderson, S., Masters, R. E., et al. (1992). *Riparian forest buffers*. Oklahoma Cooperative Extension Service. https://pods.okstate.edu/fact-sheets/NREM-5034pod-color.pdf

Arnell, N. W., & Gosling, S. N. (2016). The impacts of climate change on river flood risk at the global scale. *Climatic Change*, *134*, 387–401. https://doi.org/10.1007/s10584-014-1084-5

Asselman, N., Van Heeringen, K.-J., De Jong, J., & Geertsema, T. (2022). Juli 2021 overstroming en wateroverlast in zuid-limburg - eerste bevindingen voor valkenburg, geulmonding, roermonding en eygelshoven. *Deltares report*. https://publications.deltares.nl/11207700_000_0019.pdf

Bathurst, J. C., Birkinshaw, S. J., Cisneros Espinosa, F., & Iroumé, A. (2017). Forest impact on flood peak discharge and sediment yield in streamflow. *River System Analysis and Management*, 15–29. https://doi.org/10.1007/978-981-10-1472-7_2

Bennett, W., Horrillo-Caraballo, J., Fairchild, T., van Veelen, T. J., & Karunarathna, H. (2023). Saltmarsh vegetation alters tidal hydrodynamics of small estuaries. *Applied Ocean Research*, *138*, 103678. https://doi.org/10.1016/j.apor.2023.103678

Bhattacharjee, K., & Behera, B. (2018). Does forest cover help prevent flood damage? empirical evidence from india. *Global Environmental Change*, *53*, 78–89. https://doi.org/10.1016/j.gloenvcha.2018.09.004

Blöschl, G., Gaál, L., Hall, J., Kiss, A., Komma, J., Nester, T., Parajka, J., Perdigão, R. A., Plavcová, L., Rogger, M., et al. (2015). Increasing river floods: Fiction or reality? *Wiley Interdisciplinary Reviews: Water*, *2*(4), 329–344. https://doi.org/10.1002/wat2.1079

Bondelid, T. R., McCuen, R. H., & Jackson, T. J. (1982). Sensitivity of scs models to curve number variation 1. *JAWRA Journal of the American Water Resources Association*, *18*(1), 111–116. https://doi.org/10.1111/j.1752-1688.1982.tb04536.x

Boughton, W. (1989). A review of the usda scs curve number method. *Soil Research*, *27*(3), 511–523. https://doi.org/10.1071/SR9890511

Brauer, C. C., Teuling, A. J., Overeem, A., Van Der Velde, Y., Hazenberg, P., Warmerdam, P., & Uijlenhoet, R. (2011). Anatomy of extraordinary rainfall and flash flood in a dutch lowland catchment. *Hydrology and Earth System Sciences*, *15*(6), 1991–2005. https://doi.org/10.5194/hess-15-1991-2011

Buechel, M., Slater, L., & Dadson, S. (2022). Hydrological impact of wide-spread afforestation in great britain using a large ensemble of modelled scenarios. *Communications Earth & Environment*, *3*(1), 6. https://doi.org/10.1038/s43247-021-00334-0

Calder, I. R., & Aylward, B. (2006). Forest and floods: Moving to an evidence-based approach to watershed and integrated flood management. *Water International*, *31*(1), 87–99. https://doi.org/10.1080/02508060608691918

Carrick, J., Abdul Rahim, M. S. A. B., Adjei, C., Ashraa Kalee, H. H. H., Banks, S. J., Bolam, F. C., Campos Luna, I. M., Clark, B., Cowton, J., Domingos, I. F. N., et al. (2019). Is

planting trees the solution to reducing flood risks? *Journal of Flood Risk Management*, *12*(S2), e12484. https://doi.org/10.1111/jfr3.12484

Chakraborty, T., Biswas, T., Campbell, L. S., Franklin, B., Parker, S. S., & Tukman, M. (2022). Feasibility of afforestation as an equitable nature-based solution in urban areas. *Sustainable Cities and Society*, *81*, 103826. https://doi.org/10.1016/j.scs.2022.103826

Chen, Z., Luo, F., Zhou, G., Zhu, F., Wu, H., Li, R., & Zhang, C. (2024). Hydrodynamic modeling study of nature-based hybrid coastal defense strategy applied in salt marsh restoration. *Estuarine, Coastal and Shelf Science*, *298*, 108666. https://doi.org/10.1016/j.ecss.2024.108666

Cheng, Y., Sang, Y., Wang, Z., Guo, Y., & Tang, Y. (2021). Effects of rainfall and underlying surface on flood recession—the upper huaihe river basin case. *International Journal of Disaster Risk Science*, *12*, 111–120. https://doi.org/10.1007/s13753-020-00310-w

Cronshey, R. (1986). *Urban hydrology for small watersheds*. US Department of Agriculture, Soil Conservation Service, Engineering Division.

De Moor, J., Kasse, C., Van Balen, R., Vandenberghe, J., & Wallinga, J. (2008). Human and climate impact on catchment development during the holocene—geul river, the netherlands. *Geomorphology*, *98*(3-4), 316–339. https://doi.org/10.1016/j.geomorph.2006.12.033

Della Justina, C. R. V., Junior, J. L., Ferreira, M. I. P., & Rodrigues, P. P. G. W. (2019). Nature based solutions as a promising alternative for river restoration and flood reduction. *Boletim do Observatório Ambiental Alberto Ribeiro Lamego*, *13*(2), 198–212. http://dx.doi.org/10.19180/2177-4560.v13n22019p198-212

Di Gregorio, A. (2005). *Land cover classification system: Classification concepts and user manual: Lccs* (Vol. 2). Food; Agriculture Organization.

Dittrich, R., Ball, T., Wreford, A., Moran, D., & Spray, C. J. (2019). A cost-benefit analysis of afforestation as a climate change adaptation measure to reduce flood risk. *Journal of Flood Risk Management*, *12*(4), e12482. https://doi.org/10.1111/jfr3.12482

Doelman, J. C., Stehfest, E., van Vuuren, D. P., Tabeau, A., Hof, A. F., Braakhekke, M. C., Gernaat, D. E., van den Berg, M., van Zeist, W.-J., Daioglou, V., et al. (2020). Afforestation for climate change mitigation: Potentials, risks and trade-offs. *Global Change Biology*, *26*(3), 1576–1591. https://doi.org/10.1111/gcb.14887

EGDI. (2016). Egdi 1:1 million pan-european surface geology. https://metadata.europe-geology.eu/record/basic/5729ffdf-2558-48fc-a5d2-645a0a010855?language=eng

Eilander, D., Couasnon, A., Leijnse, T., Ikeuchi, H., Yamazaki, D., Muis, S., Dullaart, J., Haag, A., Winsemius, H. C., & Ward, P. J. (2023). A globally applicable framework for compound flood hazard modeling. *Natural hazards and earth system sciences*, *23*(2), 823–846. https://nhess.copernicus.org/articles/23/823/2023/

European Commission, E. (2024). Nature-based solutions [Accessed: 07-02-2024]. *Research and innovation*. https://research-and-innovation.ec.europa.eu/research-area/environment/nature-based-solutions_en

Glenis, V., Kutija, V., & Kilsby, C. G. (2018). A fully hydrodynamic urban flood modelling system representing buildings, green space and interventions. *Environmental Modelling & Software*, *109*, 272–292. https://doi.org/10.1016/j.envsoft.2018.07.018

Gottwald, S., Brenner, J., Janssen, R., & Albert, C. (2021). Using geodesign as a boundary management process for planning nature-based solutions in river landscapes. *Ambio*, *50*(8), 1477–1496. https://doi.org/10.1007/s13280-020-01435-4

Graziano, M. P., Deguire, A. K., & Surasinghe, T. D. (2022). Riparian buffers as a critical landscape feature: Insights for riverscape conservation and policy renovations. *Diversity*, *14*(3), 172. https://doi.org/10.3390/d14030172

Gutman, J. (2019). Commentary: Urban wetlands restoration as nbs for flood risk mitigation: From positive case to legitimate practice, in the view of evidence-based flood

risk policy making. *Nature-Based Flood Risk Management on Private Land: Disciplinary Perspectives on a Multidisciplinary Challenge*, 127–134. https://doi.org/10.1007/978-3-030-23842-1_13

Harrigan, S., Zsoter, E., Alfieri, L., Prudhomme, C., Salamon, P., Wetterhall, F., Barnard, C., Cloke, H., & Pappenberger, F. (2020). Glofas-era5 operational global river discharge reanalysis 1979–present. *Earth System Science Data*, *12*(3), 2043–2060. https://doi.org/10.5194/essd-12-2043-2020

Hartmann, T., Slavíková, L., & McCarthy, S. (2019). Nature-based solutions in flood risk management. *Nature-based flood risk management on private land: Disciplinary perspectives on a multidisciplinary challenge*, 3–8. https://doi.org/10.1007/978-3-030-23842-1_1

Hawker, L., Uhe, P., Paulo, L., Sosa, J., Savage, J., Sampson, C., & Neal, J. (2022). A 30 m global map of elevation with forests and buildings removed. *Environmental Research Letters*, *17*(2), 024016. https://iopscience.iop.org/article/10.1088/1748-9326/ac4d4f/meta

Hazeu, G., Schuiling, R., Thomas, D., Vittek, M., Storm, M., & Bulens, J. D. (2023). Landelijk grondgebruiksbestand nederland 2021 (lgn2021): Achtergronden, methodiek en validatie. https://doi.org/10.18174/585714

HEC-HMS. (2023). Creating a Curve Number Grid and Computing Subbasin Average Curve Number Values. [[Accessed 16-05-2024]].

Hendrix, P., & Meinardi, C. R. (2004). Bronnen en bronbeken van zuid-lim-burg; de kwaliteit van grondwater, bronwater en beekwater. *RIVM rapport 500003003*.

Hocini, N., Payrastre, O., Bourgin, F., Gaume, E., Davy, P., Lague, D., Poinsignon, L., & Pons, F. (2021). Performance of automated methods for flash flood inundation mapping: A comparison of a digital terrain model (dtm) filling and two hydrodynamic methods. *Hydrology and Earth System Sciences*, *25*(6), 2979–2995. https://doi.org/10.5194/hess-25-2979-2021

Hugtenburg, J., Kreulen, M., Hartveld, F., De Bijl, J., Van Winden, A., Van Waterloo, M., Meertens, H., & Rademakers, J. (2023). Water vasthouden en vertragen in het geuldal – natuur inzetten tegen wateroverlast en droogte. *Natuurkracht*. https://www.hnsland.nl/documents/83/20231206_HNS_Geuldal_rapport_definitief.pdf

Idsinga, D. (2024). *Safely building new houses in the geul catchment: How to mitigate the impact on flooding?* [Master's thesis, TU Delft]. http://resolver.tudelft.nl/uuid:79c6bd6b-d008-408b-a2ac-aef988df76e2

Jaafar, H. H., Ahmad, F. A., & El Beyrouthy, N. (2019). Gcn250, new global gridded curve numbers for hydrologic modeling and design. *Scientific data*, *6*(1), 145. https://doi.org/10.1038/s41597-019-0155-x

Johnen, G., Sapač, K., Rusjan, S., Zupanc, V., Vidmar, A., & Bezak, N. (2020). Modelling and evaluation of the effect of afforestation on the runoff generation within the glinščica river catchment (central slovenia). In *Nature-based solutions for flood mitigation: Environmental and socio-economic aspects* (pp. 215–231). Springer. https://doi.org/10.1007/698_2020_649

Kalyanapu, A. J., Burian, S. J., & McPherson, T. N. (2009). Effect of land use-based surface roughness on hydrologic model output. *Journal of Spatial Hydrology*, *9*(2). https://scholarsarchive.byu.edu/josh/vol9/iss2/2/

Kapetas, L., & Fenner, R. (2020). Integrating blue-green and grey infrastructure through an adaptation pathways approach to surface water flooding. *Philosophical Transactions of the Royal Society A*, *378*(2168), 20190204. http://dx.doi.org/10.1098/rsta.2019.0204

Klein, A. (2022). *Hydrological response of the geul catchment to the rainfall in july 2021* [Master's thesis, TU Delft]. http://resolver.tudelft.nl/uuid:ee25d687-70af-4aca-ae41-78e3f83943bf

KNMI. (2024). Knmi klimaatviewer. https://www.knmi.nl/klimaat-viewer/kaarten/neerslag-verdamping/gemiddelde-hoeveelheid-neerslag/jaar/Periode_1991-2020

Kottek, M., Grieser, J., Beck, C., Rudolf, B., & Rubel, F. (2006). World map of the köppen-geiger climate classification updated. https://dx.doi.org/10.1127/0941-2948/2006/0130

Kreienkamp, F., Philip, S. Y., Tradowsky, J. S., Kew, S. F., Lorenz, P., Arrighi, J., Belleflamme, A., Bettmann, T., Caluwaerts, S., Chan, S. C., et al. (2021). Rapid attribution of heavy rainfall events leading to the severe flooding in western europe during july 2021. *World Weather Atribution*. http://hdl.handle.net/1854/LU-8732135

Kundzewicz, Z. W. (2008). Climate change impacts on the hydrological cycle. *Ecohydrology & Hydrobiology*, *8*(2-4), 195–203. https://doi.org/10.2478/v10104-009-0015-y

Leijnse, T. (2024). Sfincs documentation - release 2.0.3 cauberg. https://sfincs.readthedocs.io/en/latest/input.html

Leijnse, T., van Ormondt, M., Nederhoff, K., & van Dongeren, A. (2021). Modeling compound flooding in coastal systems using a computationally efficient reduced-physics solver: Including fluvial, pluvial, tidal, wind-and wave-driven processes. *Coastal Engineering*, *163*, 103796. https://doi.org/10.1016/j.coastaleng.2020.103796

Leopold, L. B., & Maddock, T. (1953). *The hydraulic geometry of stream channels and some physiographic implications* (Vol. 252). US Government Printing Office.

Limburg, P. (2023, June). *Eerste concept limburgs programma landelijk gebied*. https://www.limburg.nl/onderwerpen/natuur-en-landschap/limburgs-programma-landelijk-gebied/

Lin, E., Shaad, K., & Girot, C. (2016). Developing river rehabilitation scenarios by integrating landscape and hydrodynamic modeling for the ciliwung river in jakarta, indonesia. *Sustainable Cities and Society*, *20*, 180–198. https://doi.org/10.1016/j.scs.2015.09.011

Lin, P., Pan, M., Beck, H. E., Yang, Y., Yamazaki, D., Frasson, R., David, C. H., Durand, M., Pavelsky, T. M., Allen, G. H., et al. (2019). Global reconstruction of naturalized river flows at 2.94 million reaches. *Water resources research*, *55*(8), 6499–6516. https://doi.org/10.1029/2019WR025287

Lu, P., & Sun, Y. (2023). Scenario-based hydrodynamic simulation of adaptive strategies for urban design to improve flood resilience: A case study of the mingzhu bay region, guangzhou, greater bay area. *River Research and Applications*, *39*(7), 1425–1436. https://doi.org/10.1002/rra.3913

Madsen, H., Lawrence, D., Lang, M., Martinkova, M., & Kjeldsen, T. (2014). Review of trend analysis and climate change projections of extreme precipitation and floods in europe. *Journal of Hydrology*, *519*, 3634–3650.

Manes, S., Vale, M. M., & Pires, A. P. (2024). Nature-based solutions potential for flood risk reduction under extreme rainfall events. *Ambio*, 1–14. https://doi.org/10.1007/s13280-024-02005-8

Marchi, L., Borga, M., Preciso, E., & Gaume, E. (2010). Characterisation of selected extreme flash floods in europe and implications for flood risk management. *Journal of Hydrology*, *394*(1-2), 118–133. https://doi.org/10.1016/j.jhydrol.2010.07.017

Middendorp, R. (2023). *Design of a flood bypass tunnel for valkenburg aan de geul: Operation and hydraulic design to reduce the risk of flooding* [Master's thesis, TU Delft]. http://resolver.tudelft.nl/uuid:22754f9c-cbc3-47fb-a908-a83a8ea701e8

Milly, P. C. D., Wetherald, R. T., Dunne, K., & Delworth, T. L. (2002). Increasing risk of great floods in a changing climate. *Nature*, *415*(6871), 514–517. https://doi.org/10.1038/415514a

Mohammed, M. J. (2022). *Flash flood modeling for geul catchment, considering different mitigation measures for july 2021 extrem rainfalls.* [Master's thesis, University of Twente]. https://purl.utwente.nl/essays/93857

Mölder, F., Jablonski, K. P., Letcher, B., Hall, M. B., Tomkins-Tinch, C. H., Sochat, V., Forster, J., Lee, S., Twardziok, S. O., Kanitz, A., et al. (2021). Sustainable data analysis with snakemake. *F1000Research*, *10*. https://doi.org/10.12688%2Ff1000research.29032.2

Muñoz-Sabater, J., Dutra, E., Agustí-Panareda, A., Albergel, C., Arduini, G., Balsamo, G., Boussetta, S., Choulga, M., Harrigan, S., Hersbach, H., et al. (2021). Era5-land: A state-of-the-art global reanalysis dataset for land applications. *Earth system science data*, *13*(9), 4349–4383.

Nadal-Romero, E., Llena, M., Melani Cortijos-López, M., & Lasanta, T. (2023). Afforestation after land abandonment as a nature based solution in mediterranean mid-mountain areas: Implications and research gaps. *Current Opinion in Environmental Science & Health*, 100481. https://doi.org/10.1016/j.coesh.2023.100481

Najafi, H., Shrestha, P. K., Rakovec, O., Apel, H., Vorogushyn, S., Kumar, R., Thober, S., Merz, B., & Samaniego, L. (2024). High-resolution impact-based early warning system for riverine flooding. *Nature communications*, *15*(1), 3726. https://doi.org/10.1038/s41467-024-48065-y

Nederhoff, K., Crosby, S. C., Van Arendonk, N. R., Grossman, E. E., Tehranirad, B., Leijnse, T., Klessens, W., & Barnard, P. L. (2024). Dynamic modeling of coastal compound flooding hazards due to tides, extratropical storms, waves, and sea-level rise: A case study in the salish sea, washington (usa). *Water*, *16*(2), 346. https://doi.org/10.3390/w16020346

Niazi, M. H. K., Morales Nápoles, O., & van Wesenbeeck, B. K. (2021). Probabilistic characterization of the vegetated hydrodynamic system using non-parametric bayesian networks. *Water*, *13*(4), 398. https://doi.org/10.3390/w13040398

Nyaupane, N., Bhandari, S., Rahaman, M. M., Wagner, K., Kalra, A., Ahmad, S., & Gupta, R. (2018). Flood frequency analysis using generalized extreme value distribution and floodplain mapping for hurricane harvey in buffalo bayou. *World Environmental and Water Resources Congress 2018*, 364–375. http://dx.doi.org/10.1061/9780784481400.034

Oruc Baci, N., Jafarzadegan, K., & Moradkhani, H. (2024). Improving flood inundation modeling skill: Interconnection between model parameters and boundary conditions. *Modeling Earth Systems and Environment*, *10*(1), 243–257. https://doi.org/10.1007/s40808-023-01768-5

Plantinga, A. J., & Wu, J. (2003). Co-benefits from carbon sequestration in forests: Evaluating reductions in agricultural externalities from an afforestation policy in wisconsin. *Land Economics*, *79*(1), 74–85. https://doi.org/10.2307/3147106

Ponce, V. M., & Hawkins, R. H. (1996). Runoff curve number: Has it reached maturity? *Journal of hydrologic engineering*, *1*(1), 11–19. https://doi.org/10.1061/(ASCE)1084-0699(1996)1:1(11)

Raška, P., Bezak, N., Ferreira, C. S., Kalantari, Z., Banasik, K., Bertola, M., Bourke, M., Cerdà, A., Davids, P., de Brito, M. M., et al. (2022). Identifying barriers for nature-based solutions in flood risk management: An interdisciplinary overview using expert community approach. *Journal of Environmental Management*, *310*, 114725. https://doi.org/10.1016/j.jenvman.2022.114725

Rijke, J., van Herk, S., Zevenbergen, C., & Ashley, R. (2012). Room for the river: Delivering integrated river basin management in the netherlands. *International journal of river basin management*, *10*(4), 369–382. https://doi.org/10.1080/15715124.2012.739173

Sampson, C. C., Smith, A. M., Bates, P. D., Neal, J. C., Alfieri, L., & Freer, J. E. (2015). A high-resolution global flood hazard model. *Water resources research*, *51*(9), 7358–7381. https://doi.org/10.1002/2015WR016954

Sebastian, A., Bader, D., Nederhoff, C., Leijnse, T., Bricker, J., & Aarninkhof, S. (2021). Hindcast of pluvial, fluvial, and coastal flood damage in houston, texas during hurricane

harvey (2017) using sfincs. *Natural hazards*, *109*, 2343–2362. https://doi.org/10.1007/s11069-021-04922-3

Singh, V., & Mishra, S. (2003). Soil conservation service curve number (scs-cn) methodology. vol. 42. *Springer Science Business Media.*, *10*, 978–94.

Slager, K., Becker, A., Bouaziz, L., & Kwadijk, J. (2022). Rapid assessment study on the geul river basin: Screening of flood reduction measures. *Deltares report*. https://publications.deltares.nl/Deltares235.pdf

Slager, K., de Moel, H., & de Jong, J. (2021). *Maximum flood extents limburg floods july 2021* (Version 1). 4TU.ResearchData. https://doi.org/10.4121/16817389.v1

Tembata, K., Yamamoto, Y., Yamamoto, M., & Matsumoto, K. (2020). Don't rely too much on trees: Evidence from flood mitigation in china. *Science of The Total Environment*, *732*, 138410. https://doi.org/10.1016/j.scitotenv.2020.138410

Tradowsky, J. S., Philip, S. Y., Kreienkamp, F., Kew, S. F., Lorenz, P., Arrighi, J., Bettmann, T., Caluwaerts, S., Chan, S. C., De Cruz, L., et al. (2023). Attribution of the heavy rainfall events leading to severe flooding in western europe during july 2021. *Climatic Change*, *176*(7), 90. https://doi.org/10.1007/s10584-023-03502-7

Tsendbazar, N., Li, L., Koopman, M., Carter, S., Herold, M., Georgieva, I., & Lesiv, M. (2021). Product validation report (d12-pvr) v 1.1.

Tu, M. (2006). *Assessment of the effects of climate variability and land use change on the hydrology of the meuse river basin*. Balkema Publishers. https://research.vu.nl/ws/portalfiles/portal/80382579/complete+dissertation.pdf

Uhe, P., Hawker, L., Paulo, L., Sosa, J., Sampson, C., & Neal, J. (2022). Fabdem-a 30m global map of elevation with forests and buildings removed. *EGU General Assembly Conference Abstracts*, EGU22–8994.

Van der Veen, R., & Agtersloot, R. (2021). Topafvoeren hoogwater maas juli 2021. *Uitgever: Agtersloot Hydraulisch Advies (AHA). In opdracht van Rijkswaterstaat*.

Van Dijk, Y. (2023). *Flooding problems in the catchment area of the river geul: The impact of measures on the consequences of extreme future flooding* [Master's thesis, TU Delft]. http://resolver.tudelft.nl/uuid:df228728-0944-4cc1-810c-c9c9af23dafb

Van Heeringen, K.-J., Asselman, N., Overeem, A., Beersma, J., & Philip, S. (2022). Analyse overstroming valkenburg - watersysteem-evaluatie waterschap limburg. *Deltares report*. https://publications.deltares.nl/11207700_000_0014.pdf

van Zelst, V. T., Dijkstra, J. T., van Wesenbeeck, B. K., Eilander, D., Morris, E. P., Winsemius, H. C., Ward, P. J., & de Vries, M. B. (2021). Cutting the costs of coastal protection by integrating vegetation in flood defences. *Nature communications*, *12*(1), 6533. https://doi.org/10.1038/s41467-021-26887-4

Wahl, T., Jain, S., Bender, J., Meyers, S. D., & Luther, M. E. (2015). Increasing risk of compound flooding from storm surge and rainfall for major us cities. *Nature Climate Change*, *5*(12), 1093–1097. https://doi.org/10.1038/nclimate2736

Wallis de Vries, M. F. (2010). Uitdagingen voor het beheer van lijnvormige elementen in het heuvelland. *Natuurhistorisch Maandblad*, *99*(1), 6–11.

Ward, P. J., de Ruiter, M. C., Mård, J., Schröter, K., Van Loon, A., Veldkamp, T., von Uexkull, N., Wanders, N., AghaKouchak, A., Arnbjerg-Nielsen, K., et al. (2020). The need to integrate flood and drought disaster risk reduction strategies. *Water Security*, *11*, 100070. https://doi.org/10.1016/j.wasec.2020.100070

Waterloo, M., & Gevaert, A. (2023). Stroomgebied de geul: Effectiviteit van natuurgerelateerde maatregelen ter vermindering van overstromingsrisico's. *Not published*.

Wickham, J., Stehman, S. V., Sorenson, D. G., Gass, L., & Dewitz, J. A. (2023). Thematic accuracy assessment of the nlcd 2019 land cover for the conterminous united states. *GIScience & Remote Sensing*, *60*(1), 2181143. https://doi.org/10.1080/15481603.2023.2181143

Xiao, L., Robinson, M., & O'Connor, M. (2022). Woodland's role in natural flood management: Evidence from catchment studies in britain and ireland. *Science of the Total Environment*, *813*, 151877. https://doi.org/10.1016/j.scitotenv.2021.151877

Yamazaki, D., Ikeshima, D., Sosa, J., Bates, P. D., Allen, G. H., & Pavelsky, T. M. (2019). Merit hydro: A high-resolution global hydrography map based on latest topography dataset. *Water Resources Research*, *55*(6), 5053–5073. https://doi.org/10.1029/2019WR024873

Zanaga, D., Van De Kerchove, R., Daems, D., De Keersmaecker, W., Brockmann, C., Kirches, G., Wevers, J., Cartus, O., Santoro, M., Fritz, S., et al. (2022). Esa worldcover 10 m 2021 v200. https://zenodo.org/records/7254221